Groundwater for Sustainable Development 30 (2025) 101457

Contents lists available at ScienceDirect

Groundwater for Sustainable Development

journal homepage: www.elsevier.com/locate/gsd

Research paper

Mapping groundwater dependent ecosystems potential for sustainable management of aquifers

Despoina Charchousi [a,*], Gkeralnto Kolitsi [a], Nikolaos K. Mellios [b], Maria P. Papadopoulou [a]

[a] *Laboratory of Physical Geography and Environmental Impacts, School of Rural, Surveying and Geoinformatics Engineering, National Technical University of Athens, Athens, 15773, Greece*

[b] *Civil Engineering Department, University of Thessaly, Pedion Areos, Volos, 38334, Greece*

HIGHLIGHTS

- A multicriteria method is proposed to map groundwater dependent ecosystems.
- Four objective weighting methods are evaluated.
- Validation is based on known springs locations.
- The CRITIC method provides the most reliable weight assignments.
- Spatio-temporal changes driven by climatic variability are assessed.

GRAPHICAL ABSTRACT

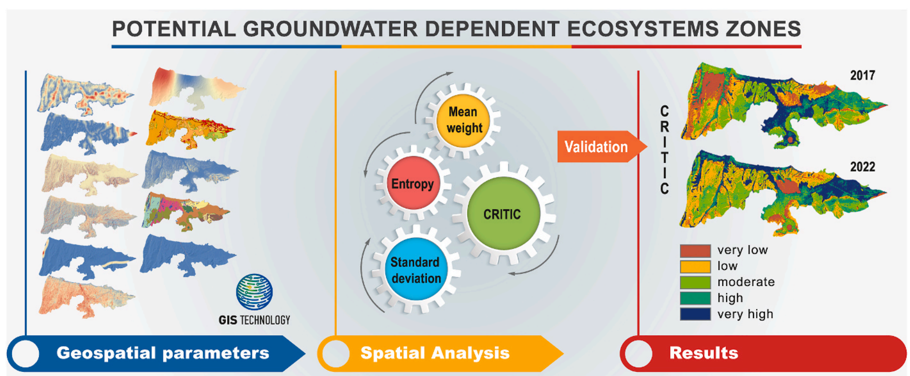

ARTICLE INFO

Keywords:
GIS-based multi-criteria approach
Objective weighting methods
entropy weighting method
Geospatial parameters
Crete

ABSTRACT

Groundwater dependent ecosystems (GDEs) mapping is critical to optimize their management and to preserve the related services. The effective use of cutting-edge technologies such as Geographic Information Systems (GIS) and remote sensing technologies is extensively proposed to facilitate GDEs mapping. This study introduces a comprehensive GDEs mapping methodology that integrates GIS and remote sensing with a multi-criteria analysis (MCA) approach. The proposed methodology aims to enhance the practicality of the existing MCA-based GDEs mapping approaches by (a) identifying a set of criteria that account for the interdependence and complementarity of inputs, and (b) specifying criteria weights via objective weighting methods to eliminate the subjective influence of experts' opinion. A coherent set of criteria is proposed as input to the developed MCA model, following a correlation assessment across a large set of parameters related to GDEs occurrence. The criteria weights are specified based on four of the most common objective weighting techniques—Mean Weight, Standard Deviation, entropy, and Criteria Importance Through Intercriteria Correlation. The proposed methodology is implemented in Chania Plain, Greece, an agricultural area characterized by a significant number of springs and a complex network of streams. The results have been validated at 13 springs; the majority of springs locations have been characterized as high to very high GDEs potential zones, with CRITIC to be proved as the most suitable

* Corresponding author.
E-mail address: charchousi@mail.ntua.gr (D. Charchousi).

https://doi.org/10.1016/j.gsd.2025.101457
Received 11 November 2024; Received in revised form 30 January 2025; Accepted 11 May 2025
Available online 12 May 2025

weighting method. The validation results highlight the suitability of the proposed set of input criteria to reliably map GDEs in a practical, time-efficient, and cost-effective manner.

1. Introduction

Groundwater serves as a vital resource covering a wide spectrum of human water needs, while playing a crucial role in sustaining ecosystems, such as karsts, springs, wetlands, woodlands, riparian forests, and baseflow rivers, collectively known as Groundwater-Dependent Ecosystems (GDEs) (Eamus et al., 2016). These ecosystems depend partially or entirely on groundwater to cover their water requirements. Eamus et al. (2006) classifies GDEs as: a) aquatic ecosystems, such as springs, wetlands, rivers, and others; b) terrestrial (vegetation-based) ecosystems; and c) subterranean ecosystems, including cave and aquifer environments. Preserving GDEs is of high importance, as they offer a wide range of benefits to humans (ecosystem services) such as climate regulation, recreation, and provision of material goods (Howard et al., 2023). Mapping GDEs is a critical step towards sustainable GDEs management and protection. However, in most cases, GDEs location information is unavailable (Howard and Merrifield, 2010; Gou et al., 2015) and although field campaigns and in-situ measurements, such as isotope analyses, may provide reliable GDEs identification, they are still quite expensive and impractical methods (Fildes et al., 2023). To bridge this gap, Geographic Information Systems (GIS) and remote sensing technologies are utilized to facilitate GDEs mapping. The integration of these technologies with multi-criteria analysis (MCA) has already gained ground in the field of groundwater management as it constitutes a well-documented technique for groundwater potential zones identification (Arulbalaji et al., 2019; Doke et al., 2021; Jhariya et al., 2021; Ejaz et al., 2024; Hairchi et al., 2024; Hulluka et al., 2024; Zewdie et al., 2024) , and it is now expanding in GDEs mapping. Literature proposes several GIS-based GDEs mapping methodologies using MCA approaches, which synthesize spatial data relevant to GDEs presence to create GDEs potential maps, presented on a likelihood scale (e.g. Duran-Llacer et al., 2022; Fildes et al., 2023). These maps do not pinpoint precise GDEs locations but instead highlight indicative zones where GDEs are expected to be met.

Table 1 summarizes various GIS-based MCA methodologies reported in literature for mapping GDEs, detailing the criteria used to identify them. Input variables for potential GDEs zone (pGDEz) models include indices related to climatic conditions (e.g. rainfall - R), topographic parameters (e.g. elevation - E), multispectral indices (e.g. Enhanced Vegetation Index – EVI), as well as geological, hydrogeological and pedological data. Commonly, experts' judgment is adopted to assign weights to these input variables, whereas validation methods demonstrating models' competency vary widely. Indicatively, validation methods such as a) field visits to identify vegetation in good health in areas characterized as very high or high probability zones of GDEs, b) already known spring locations and c) groundwater level maps are identified in the literature. It should be noted that direct validation methods of GDEs presence such as predawn leaf water potential measurements or isotope analysis are not included among the preferred ones, due to high cost and technological requirements. It is also noted that the identified GIS-based mapping methodologies are explicitly focused on terrestrial and aquatic GDEs mapping and therefore subterranean GDEs are not included on the identified pGDEz.

Following a comprehensive literature review, the present study

Table 1
GIS-based MCA GDEs mapping methodologies.

Reference		Duran-Llacer et al. (2022)	Pandey et al. (2023)	Fildes et al. (2023)	Rampheri et al. (2023)
Criteria	Elevation (**E**)	✓	✓		
	Lineament density (**Ld**)	✓	✓	✓	
	Topographic Wetness Index (**TWI**)	✓	✓		✓
	Normalized Difference Wetness Index (**NDWI**)	✓	✓		✓ (modified NDWI)
	Drainage density (**Dd**)	✓	✓		
	Geology/Lithology (**G/Lth**)	✓	✓ (both G & Lth)	✓	
	Normalized Difference Vegetation Index (**NDVI**)	✓	✓	✓	✓
	Geomorphology (**Gm**)	✓	✓		
	Rain (**R**)	✓	✓		
	Land Use and Land Cover (**LULC**)	✓	✓		✓
	Terrain Roughness Index (**TRI**)	✓			
	Topographic Position Index (**TPI**)	✓			
	Aridity Index (**AI**)	✓			
	Enhanced Vegetation Index (**EVI**)	✓			
	Flow accumulation (**Fa**)	✓			✓
	Proximity to rivers and water bodies (**Prwb**)	✓			
	Curvature (**Ct**)	✓			✓
	Slope (**Sl**)	✓			✓
	Groundwater Level (**GWL**)		✓		✓
	Normalized Difference Coefficient of Variation Index - Photosynthetic Vegetation Fractional Cover (**$NDCVI_{PVFC}$**)			✓	
	Tasseled Cap Wetness (**TCW**)			✓	
	Evapotranspiration (**ETa**)			✓	
Validation processes/ methodologies	field visits for verification of vegetation's good health	✓	✓		
	validation with groundwater level	✓	✓	✓	✓
	validation with land cover types	✓			✓
	validation with rainfall data				✓
	validation with known spring locations			✓	
Weighting method	experts judgment	✓ (Delphi method)	✓ (based on previous studies done in a similar environment and based on experts judgment)	✓ (Analytic Hierarchy Process)	✓ (Analytic Hierarchy Process)

introduces an innovative GIS-based multi-criteria analysis (MCA) approach for mapping GDEs. The proposed methodology seeks to enhance existing research by (a) systematically identifying a set of objectives and associated criteria/layers that account for the interdependence and complementarity of inputs, as well as methodology's practicality, and (b) specifying criteria weights via objective weighting methods, thus eliminating biases introduced by subjective expert judgement. To this end, this analysis incorporates four of the most common objective weighting techniques—Mean Weight (MW), Standard Deviation (SD), entropy, and Criteria Importance Through Intercriteria Correlation (CRITIC)—as highlighted by Şahin (2021). The impact of these weighting methods on the delineation of pGDEz is thoroughly evaluated. The proposed GIS-based MCA mapping methodology has been validated in a test-bed case, the Chania Plain in Crete, Greece, a region which is characterized by its agricultural landscape, where a significant group of springs (i.e. aquatic GDEs), and a complex streams network (i.e. potential GDEs) occur, providing a robust testing ground. Finally, climatic conditions' impact on the presence of GDEs is assessed by comparing GDEs areal extent between a wet and a dry year.

By addressing gaps of previous research works—i.e. the reliance on subjective expert opinions for weighting criteria and the integration of practical considerations in mapping objectives—this study contributes to the evolution of GDEs mapping methodologies, offering a more reliable and objective methodology for ecological assessment and conservation planning. Particularly, a set of interdependent and complementary criteria is proposed as inputs to the MCA, as well as objective weighting methods are adopted to prevent potential bias resulting from experts' subjectivity.

2. Validation area

Chania plain covers an area of 200 km^2 and it is located in the western part of the Region of Crete. Following approximately the natural boundaries of "Porodes Kampou Chanion" groundwater system, encoded as EL1300022 (Hellenic Republic, Ministry of Environment & Energy, Special Secretariat for water, 2024), Chania plain is characterized by extended agricultural areas, covering almost 80 % of the total area according to Copernicus Corine Land Cover 2018 (Fig. 1). The cultivations met in the area are mainly olive groves, avocados and citrus fruits. The climate of the area is Mediterranean, with mild and rainy winters and warm, dry summers; the winter period lasts from October to March, and the summer period from April to September (Steiakakis et al., 2023). In the lowlands of the area, the average minimum temperature observed in January to February, is about 9.2 °C, while the average highest temperature (30.3 °C) occurs in July (Kourgialas et al., 2019). The annual rainfall for the broader Chania area has been estimated to be 665 mm of which over 95 % occurs between October and May (Chartzoulakis et al., 2001; Goumas et al., 2017). About 65 % of the annual precipitation is lost to evapotranspiration, 21 % as runoff to sea and only 14 % recharges the groundwater (Chartzoulakis et al., 2001; Soupios et al., 2007). In Fig. 1, the numerous springs met in the area are depicted, with Agya spring considered as an ecosystem of great importance providing water supply and irrigation services (Kolitsi et al., 2024). The mean annual flow of the Agya spring is 69 hm^3; however, during summer period, the spring is limited to no outflow due to intensified pumping (Nerantzaki and Nikolaidis, 2020). The network of streams in the plain is quite complex, with Keritis and Tavronitis being the dominant rivers. The major hydrological input into Tavronitis' catchment is rainfall and consequently most of rivers' monitoring stations dry up during summer; however, springs of low capacity are met in Tavronitis' basin (Prountzos, 2013; Morianou, 2014). Keritis river is formed by Agya and Meskla springs flow and the intermittent surface runoff (Nerantzaki and Nikolaidis, 2020). Keritis River has a permanent flow only at its southern part, after the artificial lake of Agya springs as the Lake supplies the River; Keritis' upper part has an intermittent flow (FILOTIS, 2024). Groundwater availability is characterized by satisfactory quality and quantity conditions (Hellenic Republic, Ministry of Environment & Energy, Special Secretariat for water, 2024); however, due to the unequal temporal distribution of water resources and the increased demand during dry periods, water resources management is a critical factor for the area's prosperity (Kritikakis et al., 2022). Indicatively, intense irrigation needs during the dry period (April–September) contribute to mean water table decline of around 3.5 m. Additionally, groundwater flow simulations for the area, under various climate change scenarios, have shown an additional decrease of the water table of approximately 4 m, during the dry period of predicted extreme dry years (Charchousi et al., 2018).

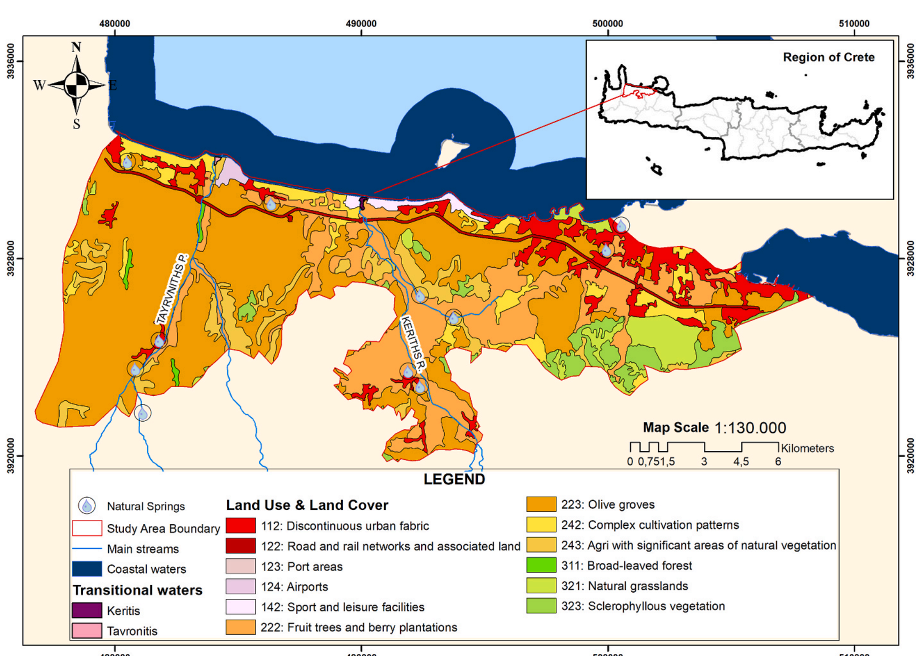

Fig. 1. Land uses, major springs and rivers in Chania Plain.

3. Methodology

3.1. Methodology's overview

In this section, the proposed methodology for potential GDEs zones (pGDEz) mapping is presented. It includes an overview on the developed methodology which consists of the following steps: a) selection of criteria related to GDEs presence, b) criteria correlation analysis via the ArcGIS Multivariate tool, c) identification of the final set of criteria by eliminating criteria that are highly correlated with other input variables, d) min-max normalization of the selected criteria, e) objective weighting methods application, f) identification of pGDEz, and g) model validation (Fig. 2). Each methodological step is analyzed thereafter.

3.2. Selection of criteria

Duran-Llacer et al. (2022) have proposed a comprehensive set of input criteria -adopted in the present study-which is the most extensive one among the reviewed methodologies of Table 1. The 18 criteria identified as predictors of GDEs presence can be classified in four categories; conventional GIS layers (e.g. Geology-G); topographic parameters (e.g. Topographic Wetness Index-TWI); multispectral indices (e.g. Normalized Difference Vegetation Index-NDVI); climate variables (e.g. Aridity Index-AI). To visualize and properly manage all input criteria, ESRI's ArcGIS Desktop 10.8.2 software has been used; a software that offers advanced mapping and spatial analysis tools (ESRI, 2024).

- **Conventional GIS layers**

The geological formations and groups (G) met in an area signify its groundwater potential and consequently GDEs potential (Duran-Llacer et al., 2022; Kabeto et al., 2022). The geological characteristics of Chania Plain (Fig. A.1) have been derived from the Geoportal of Decentralized Administration of Crete (2024). Geomorphology (Gm) constitutes also a crucial factor for pGDEz delineation (Duran-Llacer et al., 2022; Pandey et al., 2023). The Gm dataset has been obtained from the Geoportal of Greek Ministry of Environment and Energy (2024) (Fig. A.2). A Land Use and Land Cover (LULC) map offers valuable information for pGDEz identification as LULC affects hydrological phenomena such as infiltration and runoff, as well as groundwater quality, providing details on the locations of potential GDEs such as wetlands and vegetation (Pandey et al., 2023). In the present study, LULC data has been derived from CORINE Land Cover 2018 (Fig. A.3).

- **Topographic parameters**

Elevation (E) is a parameter that can impact an area's groundwater recharge potential; the higher the elevation, the smaller the groundwater potential and vice versa (Kabeto et al., 2022). Therefore, E could be considered as a criterion for pGDEz identification. Chania Plain E data have been obtained from the Copernicus Data Space Ecosystem (2024) (Fig. A.4). E has been used as unique input in ArcGIS tools for estimating slope (Sl) and curvature (Ct) (Fig. A.5 and A.6, respectively), parameters that are related to GDEs presence as they affect flow accumulation (Martínez-Santos et al., 2021; Duran-Llacer et al., 2022; Rampheri et al., 2023). Specifically, a gentle slope indicates great potential infiltration and groundwater recharge and, therefore, significant GDEs potential (Rampheri et al., 2023). In the same pattern, negative values of curvature indicate concave zones, where greater groundwater recharge and GDEs potential is expected (Duran-Llacer et al., 2022). Proximity to rivers and water bodies (Prwb) could also be considered as a parameter of GDEs identification, as riparian zones are of high potential for GDEs location (Duran-Llacer et al., 2022). In the framework of this analysis, Prwb (Fig. A.7) has been estimated via the Euclidean Distance tool in ArcGIS, using as input the rivers' network. Flow accumulation (Fa) is another criterion used in MCA GDEs mapping methodologies (Duran-Llacer et al., 2022; Rampheri et al., 2023), related to surface flow as it is used for identifying the number of cells flowing into each cell of the produced map; therefore, the higher the Fa, the greater the likelihood of GDEs (Rampheri et al., 2023). Chania Plain Fa map has been produced using the related tool in ArcGIS (Fig. A.8), which requires as input the Flow Direction raster map, also produced via ArcGIS, based on E data. Drainage density (Dd) is highly related with groundwater flow (Luijendijk, 2022); therefore, it is expected that Dd is used as a criterion for GDEs mapping (Duran-Llacer et al., 2022; Pandey et al., 2023). A relative high drainage density indicates less infiltration and, consequently, low GDEs potential (Arulbalaji et al., 2019). The Dd map of the study area (Fig. A.9) was produced via the Line Density tool of ArcGIS, using as input the Fa map. A significant lineament density (Ld) facilitates an area's infiltration and groundwater recharge rates and therefore signifies high groundwater and GDEs potential (Duran-Llacer et al., 2022; Kabeto et al., 2022; Pandey et al., 2023). In order to produce Chania Plain's Ld map (Fig. A.10), the Line Density tool of ArcGIS has been applied, using as input the faults' map provided at the Geoportal of Decentralized Administration of Crete (2024). Topographic wetness index (TWI) is widely embedded in GIS-based GDEs mapping methodologies (Duran-Llacer et al., 2022; Pandey et al., 2023; Rampheri et al., 2023; Rohde et al., 2024) as it expresses the tendency of a cell to accumulate water and therefore indicates its tendency for higher infiltration rates; thus, a greater GDEs potential. TWI is estimated based on the following Eq. (1).

$$TWI = ln\frac{\alpha}{tan\,\beta} \tag{1}$$

where α is the contributing upslope area and β is the topographic gradient at the corresponding point.

In the present study, a TWI map has been produced via ArcGIS based on Fa and Sl maps (Fig. A.11), by adapting the steps proposed in Mattivi et al. (2019). The Topographic Position Index (TPI) is an algorithm (Eq. (2)) that calculates landform gradations on topographical slope positions and is widely included in groundwater potential zones and pGDEz multi-criteria mapping methodologies (Münch and Conrad, 2007;

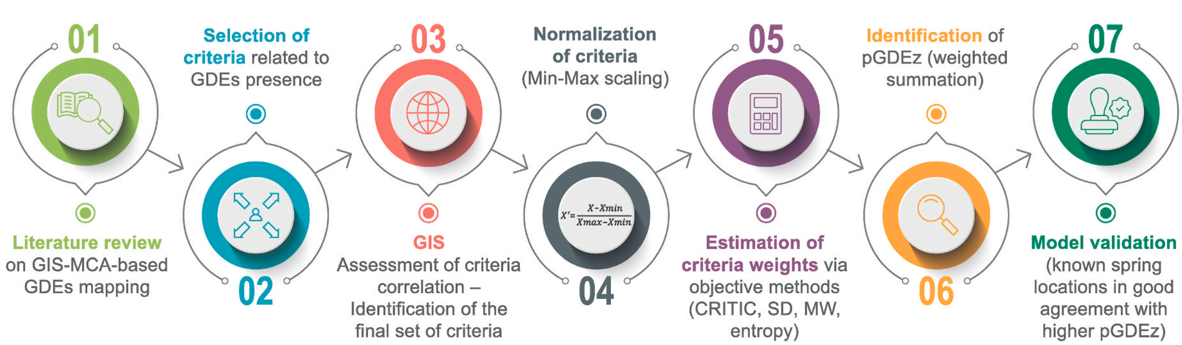

Fig. 2. The methodological steps.

Arulbalaji et al., 2019; Duran-Llacer et al., 2022; Fatema et al., 2023). Specifically, areas with high values of TPI (such as ridgetops, cliffs, mountaintops, or mid-slope) indicate low infiltration rates and therefore low GDEs potential (Fatema et al., 2023).

$$TPI = M_0 - \frac{\sum_{n-1} M_n}{n} \tag{2}$$

where M_0 is the elevation of the evaluation model point, M_n is the grid elevation and n the total number of neighboring points included in the assessment.

Chania Plain's TPI map (Fig. A.12) has been produced based on E dataset and Focal Statistic and Raster Calculator tools in ArcGIS. The Terrain Roughness Index (TRI) is a geomorphometric index that identifies and quantifies the geometry of land-surface terrain in the area under investigation and influences groundwater potential (Li et al., 2023); therefore, TRI is proposed by Duran-Llacer et al. (2022) as a predictor of pGDEz. TRI (Fig. A.13) is calculated based on Eq. (3), proposed by Riley et al. (1999), and for the present analysis the related ArcGIS tool has been applied, using E dataset as input.

$$TRI = \sqrt{\sum (x_i - x_c)^2} \tag{3}$$

where x_c is the elevation of the center cell and x_i is the elevation of each of the neighboring cells of x_c.

- **Climatic variables**

Rainfall's distribution and intensity affect runoff water and groundwater recharge and, therefore, affect groundwater potential and GDEs potential and can be used as input criteria in pGDEz mapping (Duran-Llacer et al., 2022; Pandey et al., 2023). Rainfall data retrieved from 4 local monitoring stations (Alikianos, City of Chania, Kolymvari, Platanias) have been used as input in order to produce annual rainfall maps, for the preparation for the wet year 2017 and the dry year 2022 (Fig. A.14 and A.15, respectively), based on the Inverse Distance Weightage (IDW) interpolation method available in ArcGIS. It is worth noting that the years 2017 and 2022 have been selected as typical of the wet and dry conditions, respectively, during the last decade in Chania Plain. Specifically, in 2017 the annual rainfall in the wider area ranges from 728 mm to 922 mm, while in 2022 it ranges from 518 mm to 810 mm. The United Nations Environmental Programme Aridity Index (AI) (Eq. (4)) is also proposed in the literature as a predictor of GDEs presence, since it provides information on evapotranspiration processes and rainfall deficit for potential vegetative growth (Middleton and Thomas, 1992; Gomes Marques et al., 2019; Duran-Llacer et al., 2022). A rather humid environment decreases the vegetation dependence on groundwater and, therefore, in areas with high AI, low GDEs potential is expected.

$$AI = \frac{R}{PET} \tag{4}$$

where R is the rainfall and PET is the potential evapotranspiration.

In the present analysis, temperature data from the 4 local monitoring stations have been used as input in SPEI R Package in order to estimate PET based on Thornthwaite method, as proposed by UNEP (Thornthwaite, 1948). Since the AI was calculated in the locations of the 4 monitoring stations, the IDW tool in ArcGIS has been applied to produce the Chania Plain's AI maps for the years 2017 and 2022 (Fig. A.16 and A.17, respectively). As the average temperature difference between the years 2017 and 2022 observed in the 4 meteorological stations is lower than 0.2 °C, AI follows the rainfall's pattern.

- **Multispectral indices**

The Normalized Difference Vegetation Index (NDVI) is widely used as an input in pGDEz mapping, since it provides useful information on vegetation greenness and therefore it can be used for delineating terrestrial GDEs (Gou et al., 2015; Duran-Llacer et al., 2022; Xu et al., 2022; Pandey et al., 2023; Rampheri et al., 2023). NDVI is estimated based on Eq. (5).

$$NDVI = \frac{\rho_{NIR} - \rho_{red}}{\rho_{NIR} + \rho_{red}} \tag{5}$$

where ρ_{NIR} is the spectral reflectance measurements acquired in the near-infrared region and ρ_{red} is the spectral reflectance measurements acquired in the red (visible) region.

The Enhanced Vegetation Index (EVI) is estimated based on Eq. (6) and it is also a greenness index that can be related to GDEs presence (Liu et al., 2021; Duran-Llacer et al., 2022).

$$EVI = 2.5^* \frac{\rho_{NIR} - \rho_{red}}{\rho_{NIR} + 6^*\rho_{red} - 7.5^*\rho_{blue} + 1} \tag{6}$$

where ρ_{blue} is the spectral reflectance measurements acquired in the blue region.

Another multispectral parameter that is proposed as a predictor of GDEs presence is the Normalized Difference Wetness Index (NDWI), which describes the crop's water stress level and is calculated based on Eq. (7) (Gao, 1996; Duran-Llacer et al., 2022).

$$NDWI = \frac{\rho_{NIR} - \rho_{SWIR}}{\rho_{NIR} + \rho_{SWIR}} \tag{7}$$

where ρ_{SWIR} is the spectral reflectance measurements acquired in the shortwave-infrared region.

The three multispectral indices (NDVI, EVI, NDWI) in Chania Plain have been estimated via ArcGIS raster calculator using Sentinel-2 satellite data of the wet year 2017 and dry year 2022 (Copernicus Data Space Ecosystem, 2024). Specifically, satellite images of the dry season for each studied year have been acquired, as vegetation that remains in good health during the dry season is potentially groundwater dependent (Barron et al., 2014). The generated maps depicting the multispectral indices in Chania Plain are shown in Fig. A.18-23.

3.3. Criteria correlation assessment

In order to proceed with the criteria correlation assessment, the values of the quantitative criteria (G, Gm and LULC) have been quantified using a 5-point scale, based on the following assumptions.

i) G: The criterion quantification has been based on the permeability of the geological formations. Specifically, 5 classes have been generated: 1 - impermeable geological structures, 2 - geological formations of low permeability, 3 - geological formations of moderate permeability, 4 - geological formations of high permeability, 5 - geological formations of very high permeability. The classification of the Chania Plain formations in terms of permeability has been based on the geological map of the Institute of Geology and Mineral Exploration and the final map is depicted in Fig. A.1 (Greek Ministry of Environment and Energy, 2024).

ii) Gm: In order to quantify the criterion values, the related literature has been reviewed (Duran-Llacer et al., 2022; Pandey et al., 2023) and the following classes have been adopted: 1 - dissected hills, 2 - low dissected hills, 3 - hillside, 5 - valleys with alluvial. The final reclassified map is depicted in Fig. A.2.

iii) LULC: The effect of LULC on pGDEz has been quantified by adapting the results of an experts' survey conducted by the authors' team focusing on LULC impact on groundwater contribution on environmental flow (i.e. on GDEs). The reclassification of the LULC map (Fig. A.3) has been based on the following classes: 1 – airports, ports, 2 - road and rail networks and associated land, 3 - sport and leisure facilities, discontinuous urban fabric, complex cultivation patterns, 4 - agricultural land with significant areas of natural vegetation, olive groves, fruit trees and berry plantations, 5 - broad-leaved forest, sclerophyllous vegetation, natural grasslands.

The correlation between the 18 criteria has been estimated using the ArcGIS Multivariate toolset (Duran-Llacer et al., 2022). The criteria that present correlations greater than 0.5 have been considered for elimination from the final model.

3.4. Criteria normalization

As the selected criteria are expressed in different measurement units or scales, a normalization procedure has been applied. Specifically, min–max normalization was adopted, transforming the criteria values into standard scales, which range between 0 and 1, based on Eqs. (8) and (9). Min–max normalization is a well-known normalization technique used in multi-criteria analysis (MCA) (Mhlanga and Lall, 2022), adopted in GIS-based MCA mapping methodologies (Al-Abadi et al., 2017; Meng et al., 2021).

For benefit criteria:

$$x_{ij,norm} = \frac{x_{ij} - x_{j,\min}}{x_{j,max} - x_{j,\min}} \tag{8}$$

For cost criteria:

$$x_{ij,norm} = \frac{x_{j,max} - x_{ij}}{x_{j,max} - x_{j,\min}} \tag{9}$$

where $x_{ij,norm}$ is the normalized value of the criteria j on the grid cell i, x_{ij} is the original value of the criteria j on the grid cell i, $x_{j,\ min}$ is the original minimum value of the criterion j and $x_{j,max}$ is the original maximum value of the criterion j.

3.5. Criteria weighting

- **The MW method**

The MW method assumes that all criteria are of equal importance and can be adopted in the absence of information or when the information is not sufficient (Jahan et al., 2012). Based on MW, the weights can be estimated through Eq. (10) (Odu, 2019).

$$w_{j,MW} = \frac{1}{k} \tag{10}$$

where $w_{j,MW}$ is the weight of the criterion j based on MW method and k is the total number of input criteria.

- **The SD weighting method**

To calculate criteria weights based on SD method, the following Eq. (11) is used (Odu, 2019; Mukhametzyanov, 2021).

$$w_{j,SD} = \frac{\sigma_j}{\sum_1^k \sigma_j} \tag{11}$$

where $w_{j,SD}$ is the weight of the criterion j based on the SD method and σ_j is the SD of the normalized values of criterion j.

The SD of the normalized values of each criterion derives from the relative raster's statistics.

- **The entropy weighting method**

The entropy weighting method, introduced by Shannon (1948), is based on the concept of measuring the uncertainty associated with random variables (Qu et al., 2022) and it constitutes of the following steps.

i. Criteria normalization based on Eqs. (8) and (9).
ii. Entropy estimation for criterion j based on Eq. (12).

$$H_j = -\frac{\sum_1^m \left(f_{i,j} * \ln f_{i,j}\right)}{\ln m} \tag{12}$$

where H_j is the entropy of criterion j, m is the total number of cells, and $f_{j,j}$ is the proportion of criterion j in the cell i.

In the present analysis, parameter $f_{j,j}$ has been estimated based on Eq. (13), proposed by Meng et al. (2021).

$$f_{i,j} = \frac{0.0001 + x_{ij,norm}}{\sum_1^m \left(0.0001 + x_{ij,norm}\right)} \tag{13}$$

iii. Entropy weight estimation for criterion j based on Eq. (14).

$$w_{j,ENTR} = \frac{1 - H_j}{\mathrm{k} - \sum_1^k H_j} \tag{14}$$

where $w_{j,ENTR}$ is the weight of the criterion j based on the entropy method.

- **The CRITIC weighting method**

The CRITIC weighting method, proposed by Diakoulaki et al. (1995), constitutes a widely applied objective weighting method, which addresses both the contrast intensity of each criterion (i.e. the degree of variability - SD) and the conflicting relationships between criteria (Krishnan et al., 2021). Criteria weights based on CRITIC method are estimated as follows.

i. Criteria normalization based on Eqs. (8) and (9).
ii. Estimation of the amount of information contained in criterion j based on Eq. (15).

$$C_j = \sigma_j * \sum_1^k \left(1 - r_{j,l}\right) \tag{15}$$

where C_j is the amount of information contained in criterion j and $r_{j,l}$ is the correlation coefficient between criteria j and l.

iii. CRITIC weight estimation for criterion j based on Eq. 16

$$w_{j,CRITIC} = \frac{C_j}{\sum_1^k C_j} \tag{16}$$

where $w_{j,CRITIC}$ is the weight of the criterion j based on the CRITIC method.

3.6. Final model

Since the final set of criteria has been selected and normalized and their weights have been assigned, the pGDEz map has been developed with the Spatial Analysis tool, following Eq. (17).

$$pGDEz, i = \sum_j w_{j,wm} * x_{ij,norm} \tag{17}$$

where $pGDEz,i$ is the GDEs potential in cell i and $w_{j,wm}$ is the weight of criteria j, estimated based on the indicated weighting method wm.

The values of the final map have been classified into 5 classes of GDEs potential (very low, low, moderate, high, very high), using Jenks natural breaks classification method in ArcGIS; a classification method widely applied in GIS-based MCA mapping (El-Hokayem et al., 2023; Li et al., 2023).

3.7. Model's validation

In order to assess the developed model and the impact of the weighting method on the final GDEs mapping, known spring locations -provided by Geoportal of Decentralized Administration of Crete (2024)- have been used for validation. Specifically, in spring locations, it is expected to meet zones of higher GDEs potential, as proposed by Fildes et al. (2023).

4. Results & discussion

4.1. Selection of final criteria

The selection of the final set of criteria of the multi-criteria (MCA) model is based on the correlation assessment presented in Table A.1. In alignment with existing literature, significant correlations (≥0.5) were identified among specific criteria pairs, leading to the exclusion of highly correlated parameters in the final model configuration. Specifically.

- **G-Gm-Dd correlation**: In the present analysis, Geomorphology (Gm) showed strong correlations with Geology (G) and Drainage density (Dd) (r = 0.69 and 0.52, respectively), and therefore it is discarded from the final model (Eq. (17)). Geomorphological characteristics of an area, created by geological processes, have a major influence on landslides and are determined by the lithologic properties of that area (Guhananth et al., 2023). Additionally, Gm is expected to show high correlation with Dd, as Dd is an index of fluvial geomorphology and is correlated with valley density according to the literature (Rai et al., 2017; Gao et al., 2022).
- **E-Sl-TRI correlation**: In the Chania Plain, a significant correlation has been identified between Elevation (E) and Slope (Sl) (r = 0.54), E and Terrain Roughness Index (TRI) (r = 0.56), TRI and Sl (r = 0.98). In general, the relationship of E and Sl is considered region-specific, and their correlation commonly ranges between −0.50 and + 0.50, while their relationship is parabolic (Evans and Cox, 1999). Therefore, the identified correlation level among E and Sl in Chania Plain (r = 0.54) is very close to the general upper limit (0.50). Considering that (a) in the specific analysis E is correlated with the other two variables, and (b) there is a general relationship between E and Sl -even parabolic, it is proposed to exclude E from the final model. The relationship between Sl and TRI is supported by literature; in Habib (2021) and Trevisani et al. (2023), TRI is highly correlated with Sl. In the present analysis, Sl has been selected as an input to the final model, since, according to the literature review in Choudhary et al. (2023), Sl is more commonly met on MCA groundwater potential zones mapping methodologies.
- **Ct-TPI correlation**: Topographic Position Index (TPI) is significantly correlated with the related Curvature (Ct) (r = 0.57); an expected finding since both measure terrain concavity and convexity. Among the two variables, TPI has been selected as input criteria to the final model as, according to Minár et al. (2020), curvature-related morphometric variables, such as TPI, are reported in the literature as more successful than Ct.
- **NDVI-EVI-NDWI correlation**: The multispectral indices in Chania Plain present high correlation with each other (r > 0.70) both for the wet (2017) and the dry (2022) year under study. The high correlation between Normalized Difference Vegetation Index (NDVI) and Enhanced Vegetation Index (EVI) has been expected as both indices quantify vegetation greenness; however, EVI corrects for some atmospheric conditions and canopy background noise and with improved sensitivity in dense vegetation areas (U.S. Geological Survey, 2024). Additionally, high NDVI-EVI coefficients values are reported widely in literature (e.g. Alademomi et al., 2020; Bari et al., 2021; Lykhovyd et al., 2023). NDVI and Normalized Difference Wetness Index (NDWI), although focusing on vegetation density and on vegetation water content respectively, are both used for monitoring plants health and therefore it is expected to be correlated. Consequently, a strong relationship among NDVI and NDWI is reported in the literature (e.g. Bhattacharya et al., 2021; Strashok et al., 2022). Among the examined multispectral indices, NDVI has been included in the final model, since it is considered the most popular and widely applied index used for vegetation assessment (Huang et al., 2021) and is also included in all MCA mapping methodologies of Table 1.
- **R-AI correlation**: Rainfall R and aridity index (AI) present significant correlation for both years under study, as also reported in literature (Sharma and Patel, 2024).

Therefore, the final set of criteria consists of the following 11 parameters: G, LULC, Sl, Prwb, Fa, Dd, Ld, TWI, TPI, AI, and NDVI.

4.2. Criteria weighting

Table 2 details the criteria weights and rankings derived from the 4 objective weighting methods (MW, Entropy, SD, CRITIC) across 2017 and 2022. Geology (G) consistently emerged as the predominant factor influencing GDEs presence at an area, followed by the criterion AI. G is also considered as the most important factor in Duran-Llacer et al. (2022) proposed model, for which experts' opinion has been used as a weighting method. Conversely, based on Entropy-based weights, no criterion is clearly ranked as more important. However, entropy, SD, and CRITIC methods rank flow accumulation (Fa) as the least important criterion, with the lowest relative weight.

4.3. pGDEz mapping

Figs. 3 and 4 illustrate the GDEs potential maps generated for 2017 and 2022, respectively. These maps, quantified in Fig. 5 which presents the areal extent of each pGDEz, showcase a prevalence of low to moderate potential GDEs zones in Chania Plain, stable across the weighting methods. Very high pGDEz % coverage for the year 2017 ranging from 10.3 % to 17.3 % according to the weighting method used, while for the year 2022 the relative percentage ranges from 10.3 % to 20.6 %. Comparing the areal extent of pGDEz of the wet and the dry year, the MW method does not identify variance on very high pGDEz; on the contrary, Entropy, SD and CRITIC methods identify an increase of 1.2–4.2 % -depending on the weighing method-in the very high pGDEz of the dry year 2022 compared to the wet year 2017. This finding follows the pattern indicated in Duran-Llacer et al. (2022), where also an increased coverage of the higher pGDEz during the relative drier year is observed. The aforementioned result is rather expected as the more rainfall, the lower the probability of GDEs presence (Duran-Llacer et al., 2022).

4.4. Model's validation

As previously described, the validation of the developed model has been carried out by comparing the resulting potential GDEs zone (pGDEz) with spring locations. Table 3 summarizes the model's performance for the years 2017 and 2022 and for the 4 weighting methods, compared to the known springs' locations. Based on the results depicted in Table 3, a high level of model reliability is revealed for all the weighting methods reviewed, as in all cases, none of the springs are located in very low pGDEz and only one is assigned to low pGDEz. However, CRITIC method concludes to the most reliable results with the

Table 2
Weights (W) and Rankings (Ra) of criteria based on the MW, the Entropy, the SD, and the CRITIC weighting methods.

Weighting Method	MW				Entropy				SD				CRITIC			
Year	2017		2022		2017		2022		2017		2022		2017		2022	
Criteria	W (%)	Ra	W (%)	Ra	W (%)	Ra	W (%)	Ra	W (%)	Ra	W (%)	Ra	W (%)	Ra	W (%)	Ra
Fa	9.1	1	9.1	1	6.8	11	6.8	11	2.3	11	2.3	11	2.2	11	2.2	11
Sl	9.1	1	9.1	1	9.8	3	9.8	3	5.1	9	5.1	9	5.1	9	5.1	9
Dd	9.1	1	9.1	1	9.8	5	9.8	5	11.4	3	11.4	3	12.2	3	11.9	3
TPI	9.1	1	9.1	1	9.8	2	9.8	2	2.3	10	2.3	10	2.3	10	2.2	10
Ld	9.1	1	9.1	1	7.6	9	7.6	9	7.8	7	7.8	7	8.0	6	7.6	7
G	9.1	1	9.1	1	9.6	8	9.6	8	23.1	1	23.1	1	23.5	1	23.4	1
Prwb	9.1	1	9.1	1	9.8	1	9.8	1	6.3	8	6.3	8	6.1	8	6.1	8
TWI	9.1	1	9.1	1	9.7	6	9.7	7	8.9	5	8.9	5	8.6	5	8.6	5
LULC	9.1	1	9.1	1	7.6	10	7.6	10	9.6	4	9.6	4	9.4	4	9.5	4
NDVI	9.1	1	9.1	1	9.8	4	9.8	4	8.2	6	7.8	6	7.8	7	8.1	6
AI	9.1	1	9.1	1	9.7	7	9.7	6	15.0	2	15.4	2	14.8	2	15.3	2

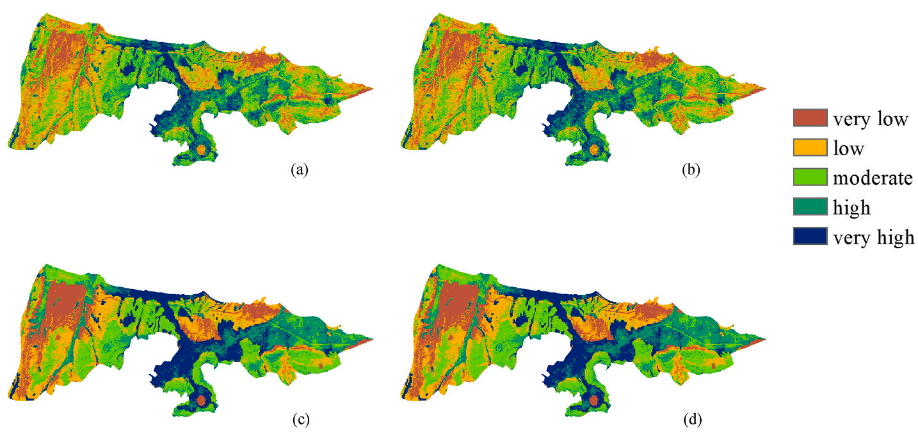

Fig. 3. Likelihood of GDEs presence in Chania Plain, based on the MW (a), the entropy (b), the SD (c), and the CRITIC (d) weighting methods, for the year 2017.

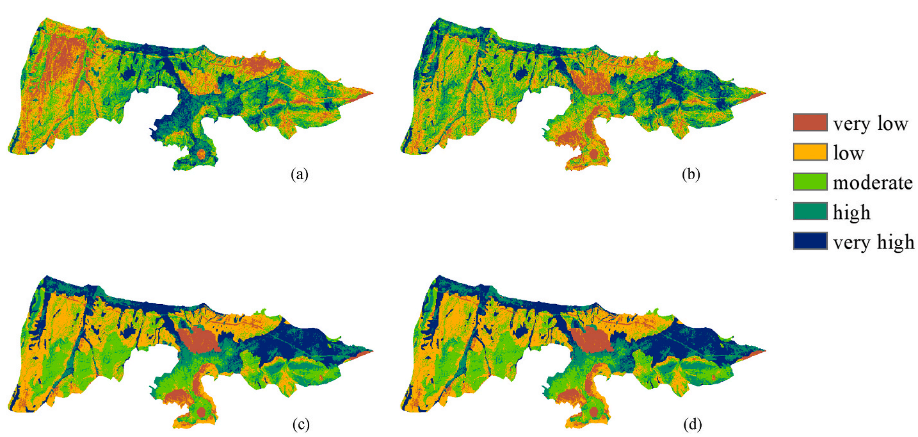

Fig. 4. Likelihood of GDEs presence in Chania Plain, based on the MW (a), the entropy (b), the SD (c), and the CRITIC (d) weighting methods, for the year 2022.

higher average percentage of springs locations on high and higher potential zones for the two examined years (85 % in year 2017 and 69 % in year 2022). The validation percentage values are comparable to those (76.5 in higher, 8.8 % in moderate, 8.8 % in low, and 5.9 % in no pGDEz) reported in Fildes et al. (2023). It is worth noting that the model has been proved more reliable in the wet year, a fact that can be interpreted by the climatic characteristics of the study area and the adopted normalization procedure. Specifically, three of the known springs' locations are classified as high to very high pGDEz in the wet year (2017), whereas as moderate zones in the dry year (2022). This differentiation could be explained by the spatial variability of Aridity Index (AI), which is wider in the dry year ($0.6 \leq AI_{2022} \leq 0.9$) compared to the AI spatial variability of the wet year ($0.8 \leq AI_{2017} \leq 1.0$). Therefore, via the normalization procedure, locations characterized by high AI values both in the dry and the wet year ($\Delta AI \leq 11$ %) are assigned in varying pGDEz. However, the methodology satisfactorily predicts the location of pGDEz in both wet and dry years as the majority of the existing springs were characterized at least of moderate GDEs potential in both cases.

As observed in Table 1, another popular methodology for validating GIS-based GDEs mapping models is the comparison of the groundwater table with the identified pGDEz. As reported in the literature, shallow groundwater table indicates higher likelihood of GDEs presence (Eamus et al., 2016; Liu et al., 2021; Xu et al., 2022); specifically, considering the complexity of the plant root systems (i.e. terrestrial GDEs) and the

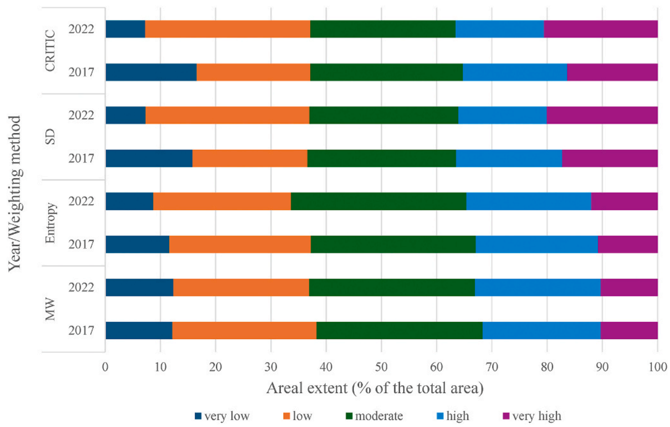

Fig. 5. Areal extent (% of the total area) of the pGDEz produced based on the MW, the Entropy, the SD, and the CRITIC weighting methods.

difficulty to quantify the rooting depth, water table depth less than 20 m can be used as an indicator of potential GDEs (Liu et al., 2021; Rampheri et al., 2023). However, Xu et al. (2022) rather question the specific validation methodology as they highlight the fact that root systems of even 32m depth have been reported in the literature, and, additionally, groundwater may affect vegetation by acting on other types of water (e.g. capillary upwelling). For the sake of completeness of the present analysis, the CRITIC-based model's results -i.e. the most reliable ones based on the known springs locations validation procedure-have been further validated based on groundwater level (GWL) data; GWL data for 4 monitoring stations and for the year 2017, provided by Decentralized Administration of Crete, have been compared to the pGDEz identified based on the CRITIC method. Based on the results presented in Table A.2, three of the monitoring stations are located in shallow groundwater areas and the specific locations have been characterized as moderate to very high pGDEz. The fourth monitoring station (HSGME) is located in deep groundwater (~35 m groundwater table depth); however, the model has assigned the characterization of high pGDEz in the location. Considering that HSGME monitoring station is located in Agya Lake's Park and surrounded by the Agya's springs complex, the probability of the model's accuracy should be considered as the area's vegetation may be affected by the capillary zone, as proposed by Xu et al. (2022).

5. Conclusions

This study introduces a comprehensive GIS-based multi-criteria analysis (MCA) methodology for mapping the potential presence of groundwater-dependent ecosystems (GDEs), representing a significant advancement in sustainable aquifer management. This approach aims to overcome the challenges associated with subjective weighting methods (Odu, 2019; Şahin, 2021), such as the biases and inefficiencies inherent in methods like Analytic Hierarchy Process (AHP) and the Delphi method. The research consistently performed a correlation assessment across a large set of parameters related to GDEs presence, ultimately selecting a refined set of input criteria for the proposed GIS-based MCA model: Geology (G), Land Use and Land Cover (LULC), Slope (Sl), Proximity to Water Bodies (Prwb), Flow Accumulation (Fa), Drainage density (Dd), Lineament density (Ld), Topographic Wetness Index (TWI), Topographic Position Index (TPI), Aridity Index (AI), and Normalized Difference Vegetation Index (NDVI). The evaluation of these criteria weights using four objective methods established that the CRITIC method provides the most reliable weight assignments, applicable across varied climatic conditions such as wet and dry years.

The validation results reinforce the suitability of the proposed set of input criteria and the CRITIC weighting method in mapping the likelihood of GDEs in a practical, time-efficient, and cost-effective manner. This approach underscores the significant variability in GDEs areal extent over time, emphasizing the necessity of annual monitoring to capture the spatio-temporal changes driven by climatic variability and human activities. Such insights are crucial for adaptive management strategies that ensure ecological sustainability and water resource preservation.

The proposed methodology offers considerable potential for transferability to other geographical areas. This is supported by the availability of fundamental input layers for environmental management or by leveraging remote sensing datasets that are easily computed. Moreover, the adaptability of the CRITIC method to easily determine criteria weights for different areas helps in eliminating the subjectivity factor, enhancing the model's applicability in diverse settings.

However, to further strengthen the robustness of this model, it is recommended that future studies apply this methodology in regions with varying climatic, hydrological, and geological characteristics. This expansion will test the universal applicability and reliability of the model under different environmental scenarios. Despite these considerations, the proposed model constitutes a powerful tool towards developing a comprehensive GDEs monitoring system, particularly in areas where obtaining in-situ data presents significant challenges. Its implementation could significantly advance our ability to manage groundwater resources sustainably and protect dependent ecosystems from the burgeoning impacts of global climate change and anthropogenic pressures. To this end, this study not only contributes to the academic discourse on groundwater management but also offers practical solutions for policymakers and practitioners focused on preserving vital ecological services and maintaining fundamental environmental services.

Glossary

AHP	Analytic Hierarchy Process
AI	Aridity Index
CRBMP	River Basin Management Plan of Crete
CRITIC	Criteria Importance Through Intercriteria Correlation
Ct	Curvature
Dd	Drainage density
E	Elevation
ETa	Evapotranspiration
EVI	Enhanced Vegetation Index
Fa	Flow accumulation
G	Geology
GDEs	Groundwater-Dependent Ecosystems
GIS	Geographic Information Systems
Gm	Geomorphology
GWL	Groundwater level
IDW	Inverse Distance Weightage

(*continued on next page*)

Table 3
Springs per pGDEz category—actual and percentage values—produced based on the MW, the Entropy, the SD, and the CRITIC weighting methods.

Springs per zone	MW		Entropy		SD		CRITIC	
	2017	2022	2017	2022	2017	2022	2017	2022
No of springs on low pGDEz	1 (8 %)	0 (0 %)	1 (8 %)	1 (8 %)	1 (8 %)	0 (0 %)	1 (8 %)	0 (0 %)
No of springs on moderate pGDEz	2 (15 %)	7 (54 %)	2 (15 %)	5 (42 %)	1 (8 %)	5 (38 %)	1 (8 %)	4 (31 %)
No of springs on high pGDEz	7 (54 %)	4 (31 %)	7 (54 %)	5 (42 %)	6 (46 %)	5 (38 %)	6 (46 %)	6 (46 %)
No of springs on very high pGDEz	3 (23 %)	2 (15 %)	3 (23 %)	1 (8 %)	5 (38 %)	3 (23 %)	5 (38 %)	3 (23 %)

(*continued*)

Ld	Lineament density
Lth	Lithology
LULC	Land Use and Land Cover
MCA	Multi-criteria analysis
MW	Mean Weight
NDCVI	Normalized Difference Coefficient of Variation Index
NDVI	Normalized Difference Vegetation Index
NDWI	Normalized Difference Wetness Index
PET	Potential Evapotranspiration
pGDEz	Potential Groundwater-Dependent Ecosystems (GDEs) Zone
Prwb	Proximity to rivers and water bodies
PVFC	Photosynthetic Vegetation Fractional Cover
R	Rain
Ra	Ranking
SD	Standard Deviation
Sl	Slope
TCW	Tasseled Cap Wetness
TPI	Topographic Position Index
TRI	Terrain Roughness Index
TWI	Topographic Wetness Index
W	Criteria weight

CRediT authorship contribution statement

Despoina Charchousi: Writing – original draft, Methodology, Investigation, Formal analysis, Conceptualization. **Gkeralnto Kolitsi:** Writing – original draft, Investigation, Formal analysis. **Nikolaos K. Mellios:** Writing – review & editing, Investigation, Formal analysis. **Maria P. Papadopoulou:** Writing – review & editing, Supervision, Methodology, Conceptualization.

Declaration of competing interest

The authors declare that they have no known competing financial interests or personal relationships that could have appeared to influence the work reported in this paper.

Acknowledgements

Part of the work described in this paper has been conducted within the NEXOGENESIS project. This project has received funding from the European Union's Horizon 2020 research and innovation programme under Grant Agreement No. 101003881.

Appendix

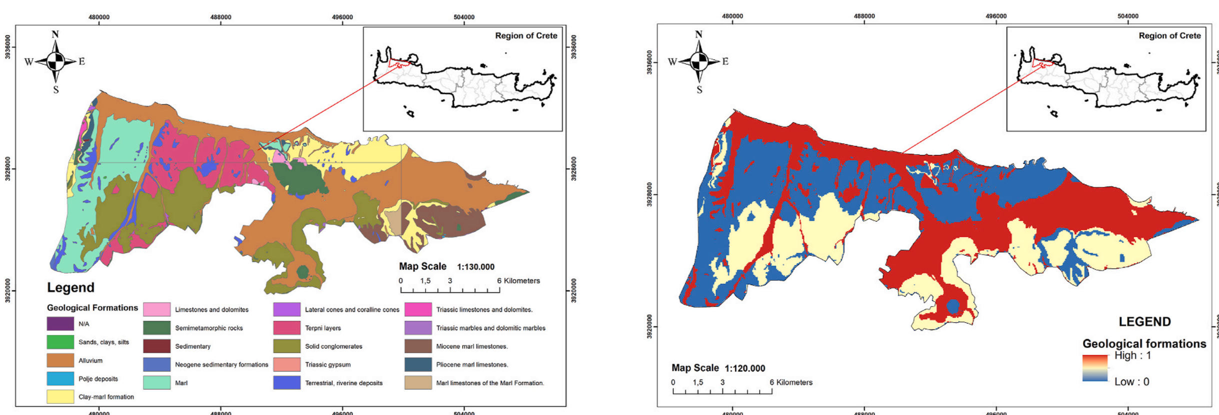

(a) (b)

Fig. A.1. (a) Chania Plain Geological formations and groups (G) map and (b) the related reclassified map

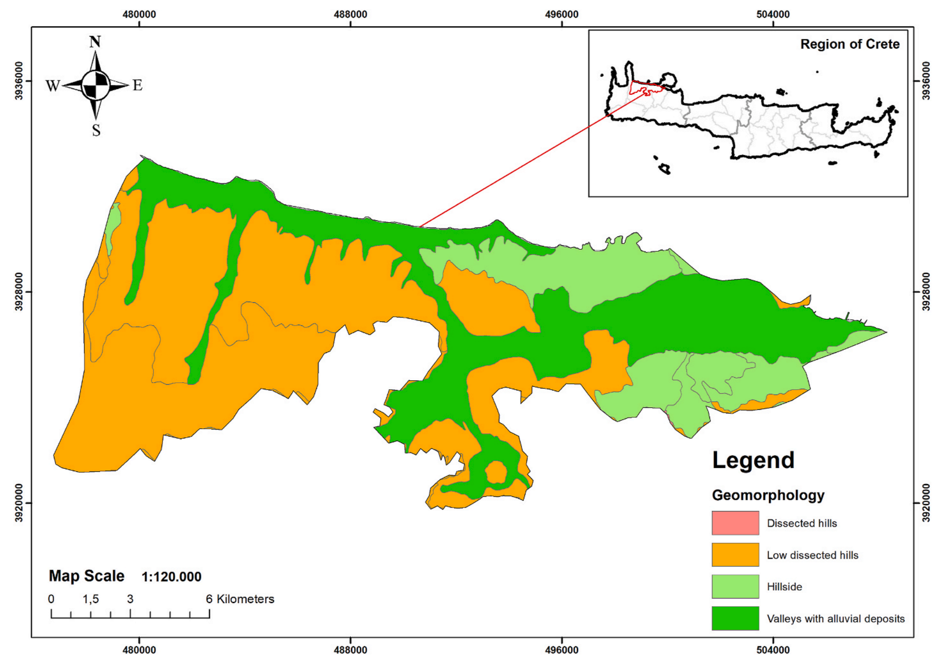

Fig. A.2. Chania Plain Geomorphology (Gm) map

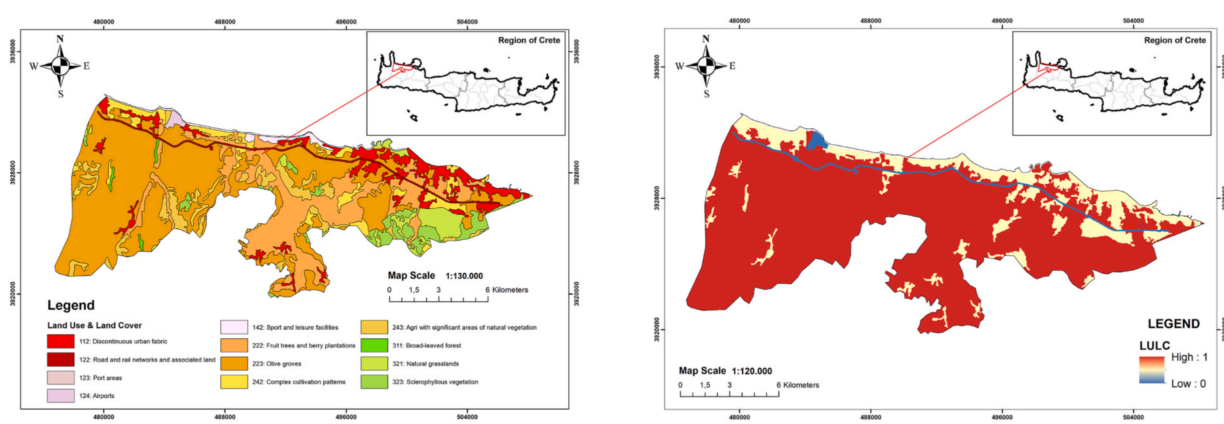

(a) (b)

Fig. A.3. (a) Chania Plain Land Use and Land Cover (LULC) map and (b) the related reclassified map

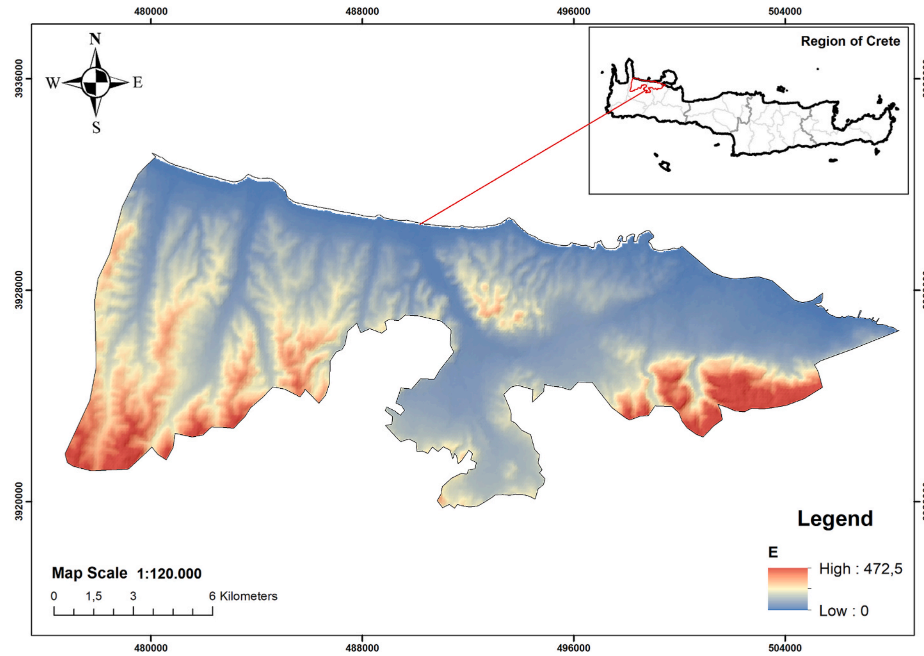

Fig. A.4. Chania Plain Elevation (E)

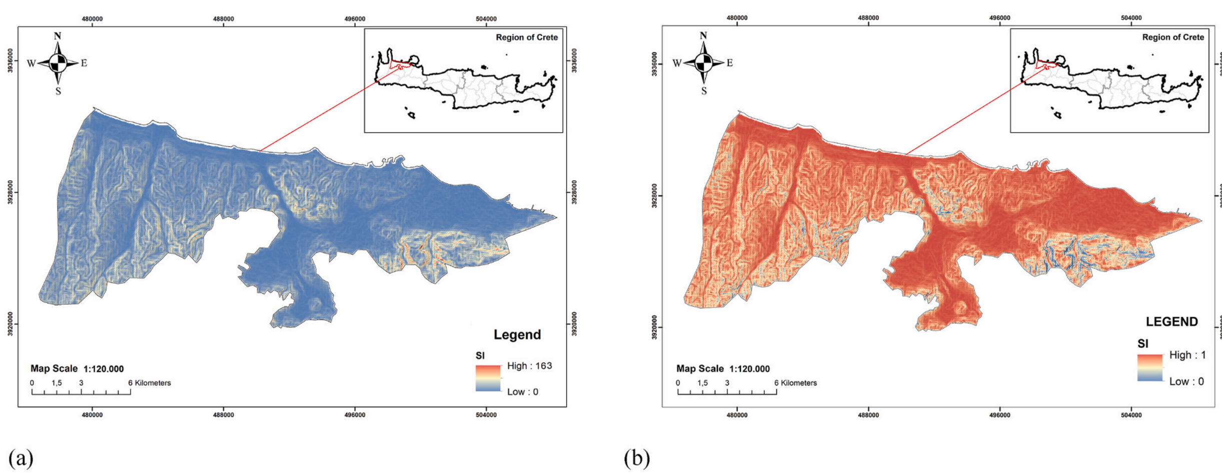

Fig. A.5. (a) Chania Plain Slope (Sl) map and (b) the related reclassified map

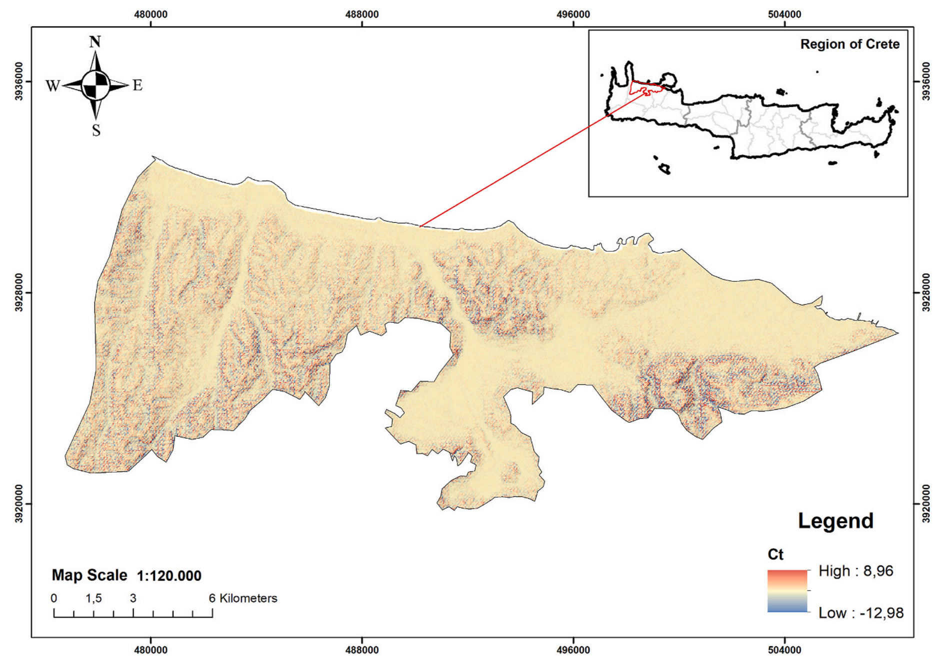

Fig. A.6. Chania Plain Curvature (Ct) map

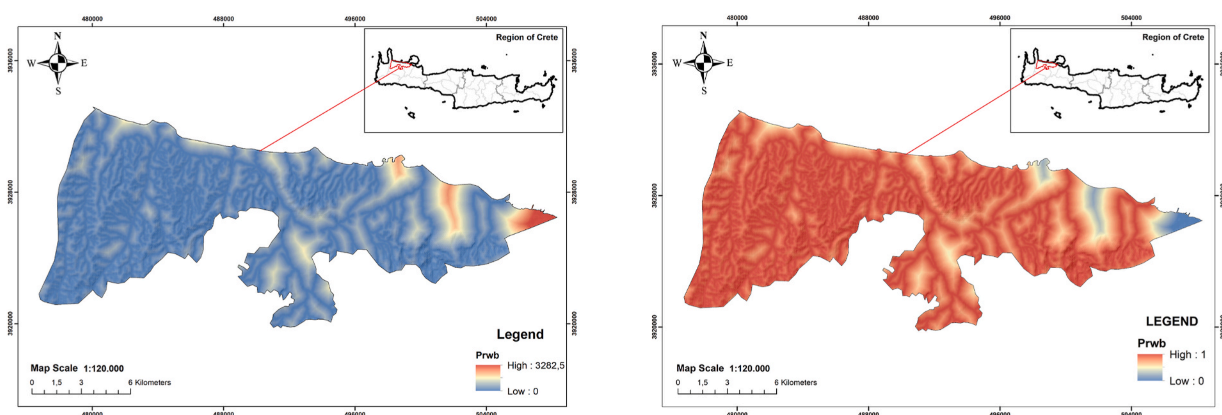

(a) (b)

Fig. A.7. (a) Chania Plain Proximity to water bodies (Prwb) map and (b) the related reclassified map

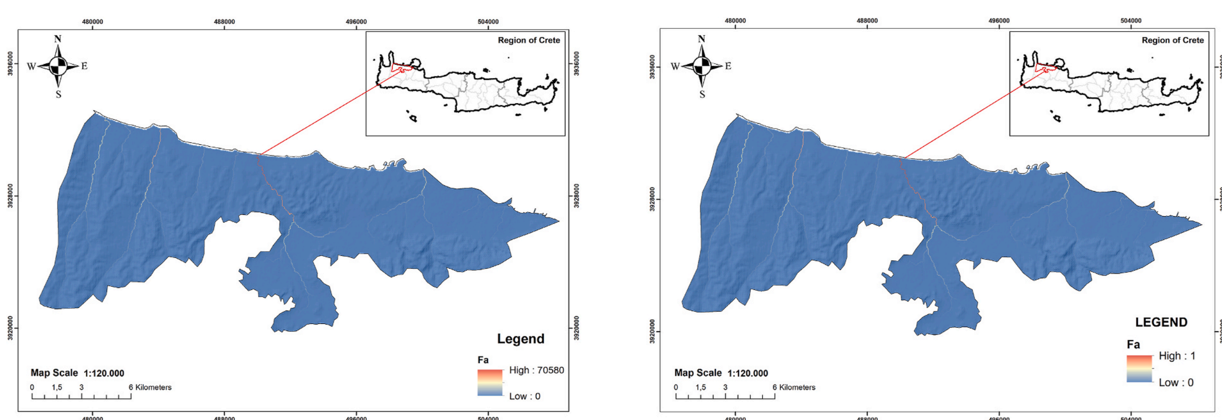

(a) (b)

Fig. A.8. (a) Chania Plain Flow accumulation (Fa) map and (b) the related reclassified map

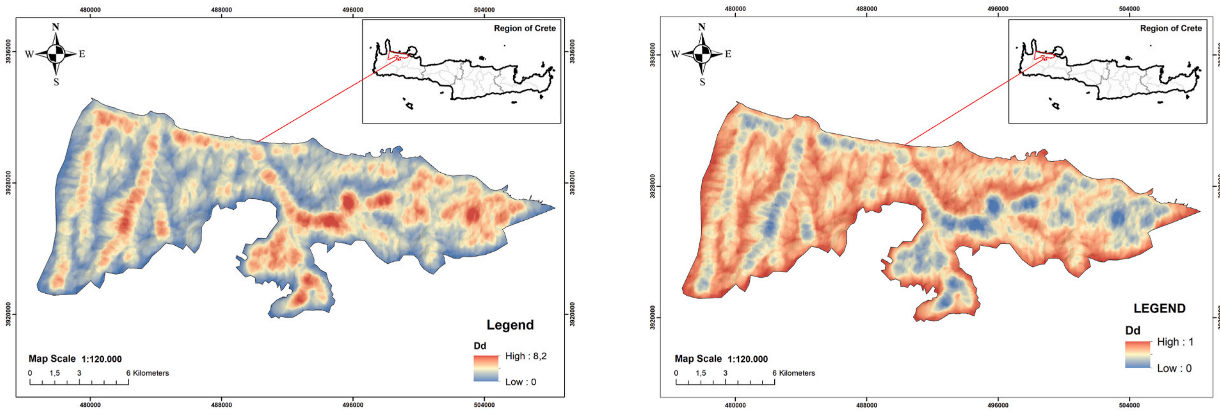

(a) (b)

Fig. A.9. (a) Chania Plain Drainage density (Dd) map and (b) the related reclassified map

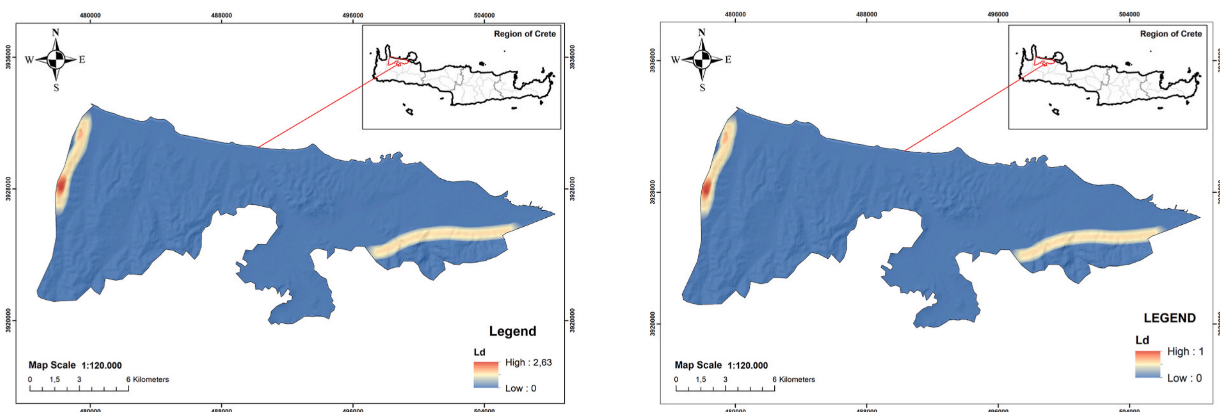

(a) (b)

Fig. A.10. (a) Chania Plain Lineament density (Ld) map and (b) the related reclassified map

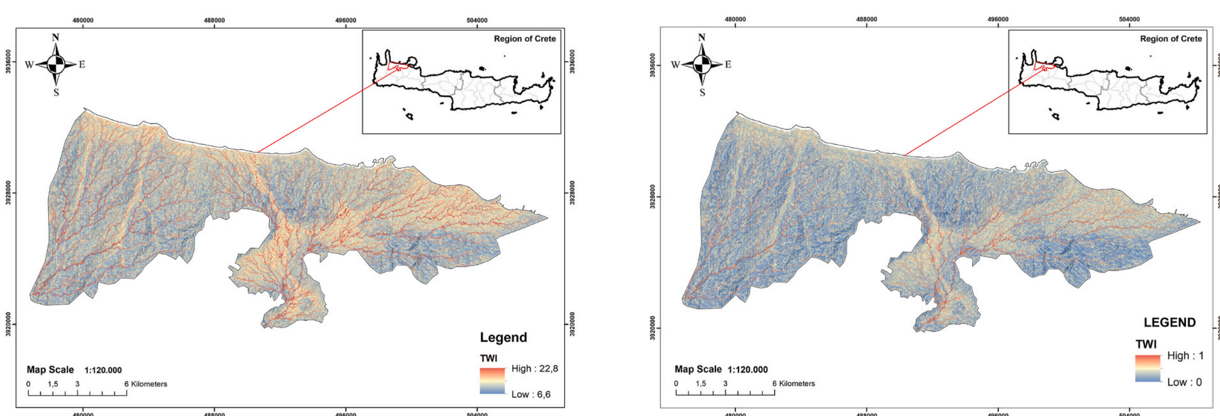

(a) (b)

Fig. A.11. (a) Chania Plain Topographic Wetness Index (TWI) map and (b) the related reclassified map

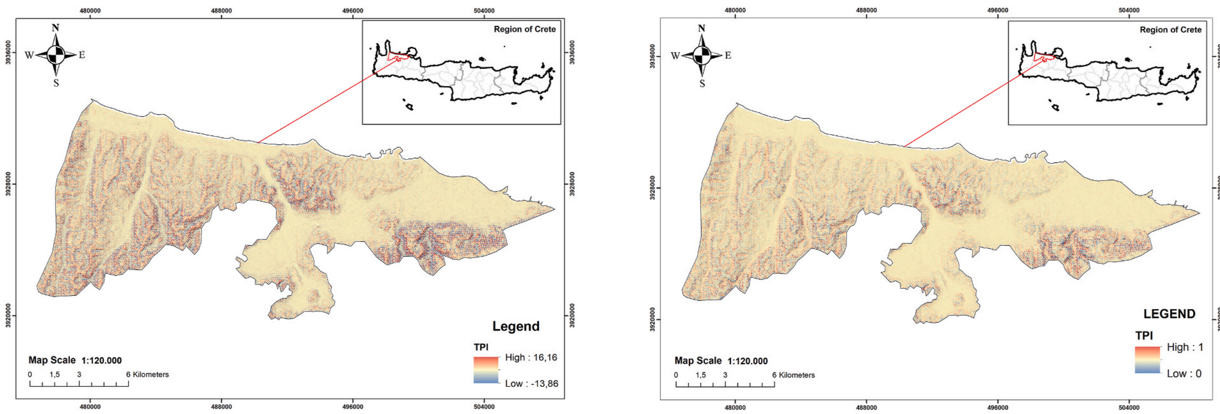

(a) (b)

Fig. A.12. (a) Chania Plain Topographic Position Index (TPI) map and (b) the related reclassified map

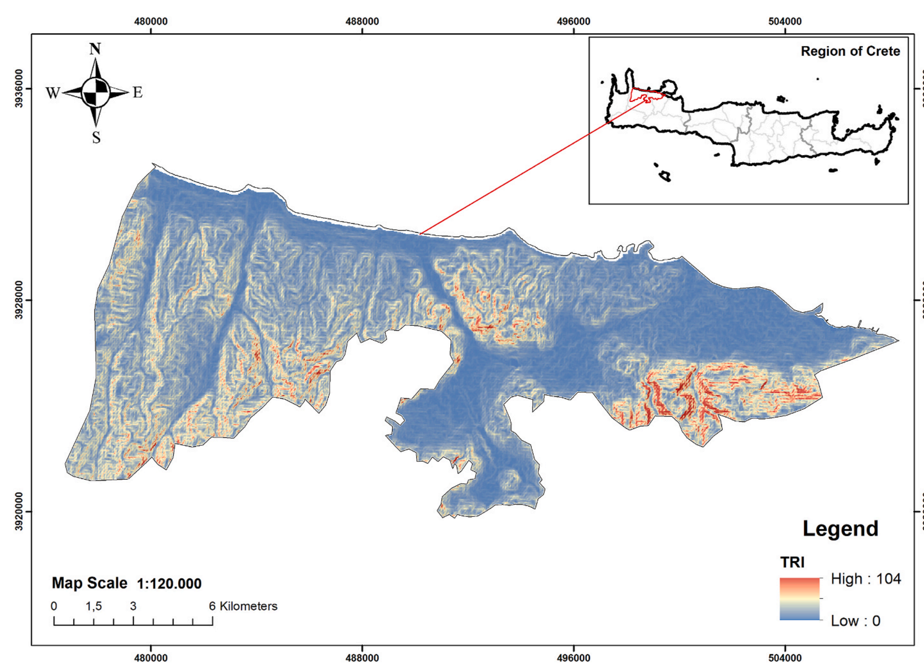

Fig. A.13. Chania Plain Terrain Roughness Index (TRI) map

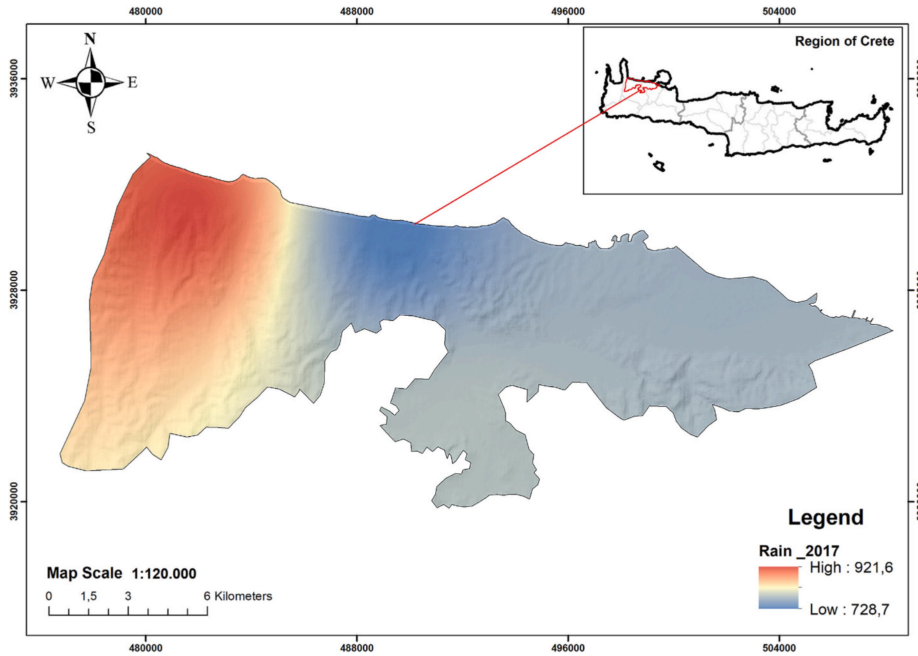

Fig. A.14. Chania Plain rainfall (R) map in 2017

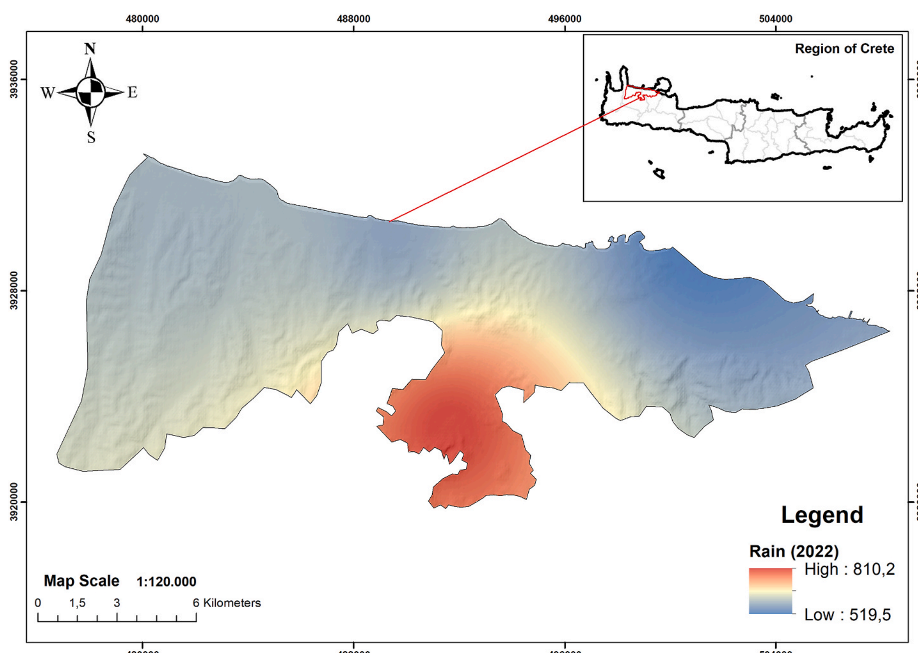

Fig. A.15. Chania Plain rainfall (R) map in 2022

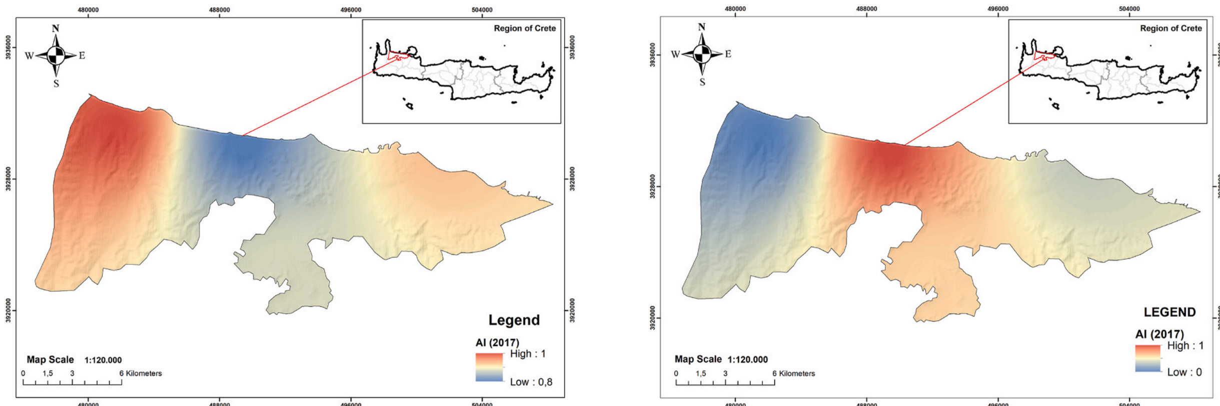

(a) (b)

Fig. A.16. (a) Chania Plain Aridity Index (AI) map and (b) the related reclassified map in 2017

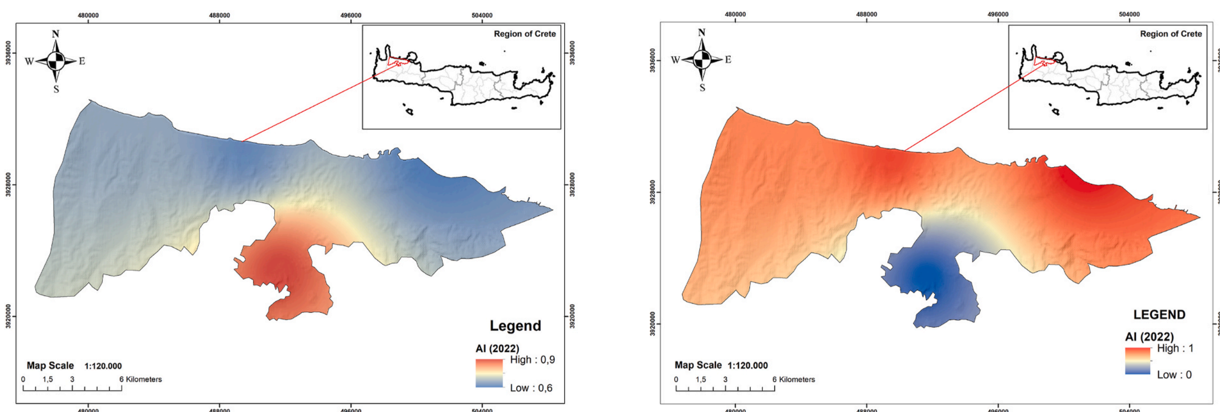

(a) (b)

Fig. A.17. (a) Chania Plain Aridity Index (AI) map and (b) the related reclassified map in 2022

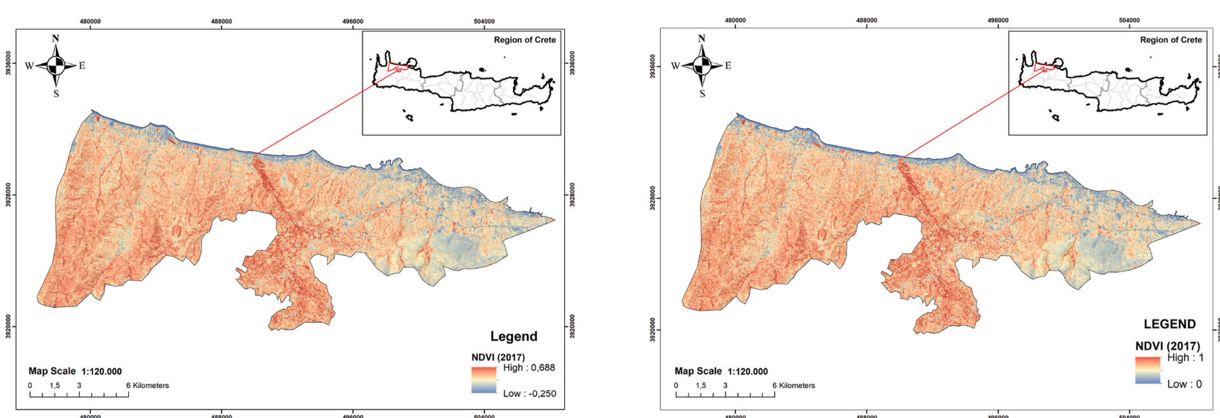

(a) (b)

Fig. A.18. (a) Chania Plain Normalized Difference Vegetation Index (NDVI) map and (b) the related reclassified map in 2017

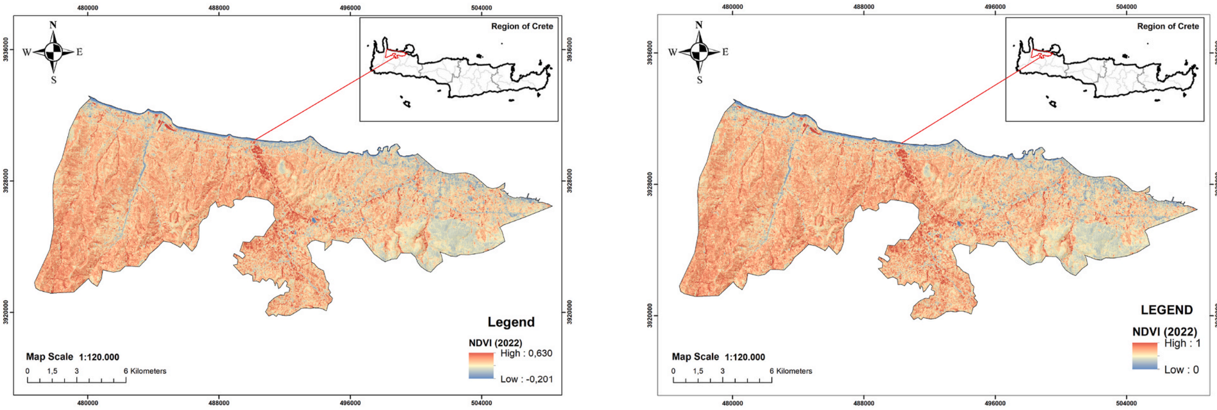

(a) (b)

Fig. A.19. (a) Chania Plain Normalized Difference Vegetation Index (NDVI) map and (b) the related reclassified map in 2022

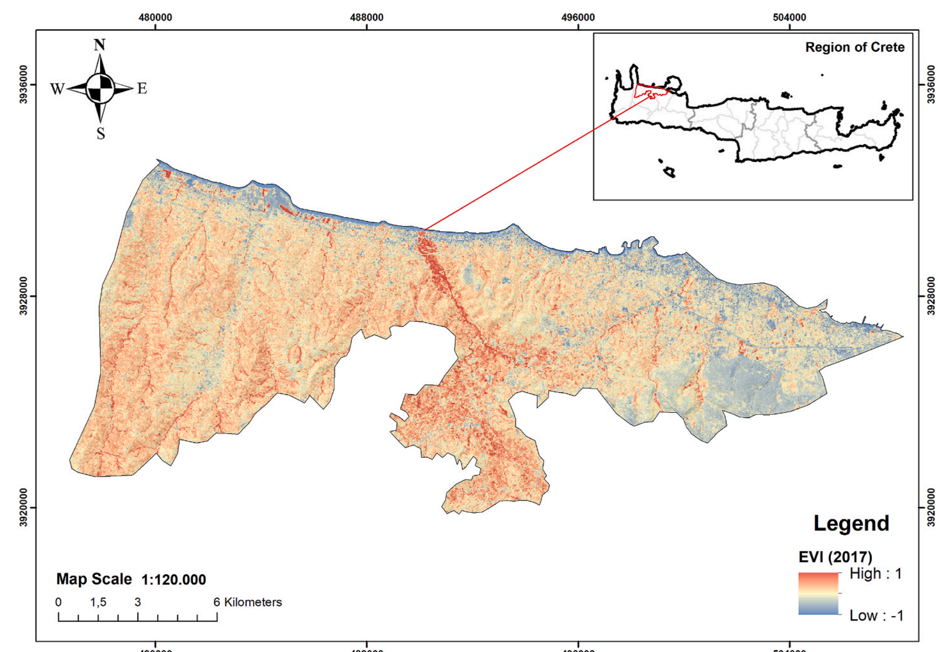

Fig. A.20. Chania Plain Enhanced Vegetation Index (EVI) map in 2017

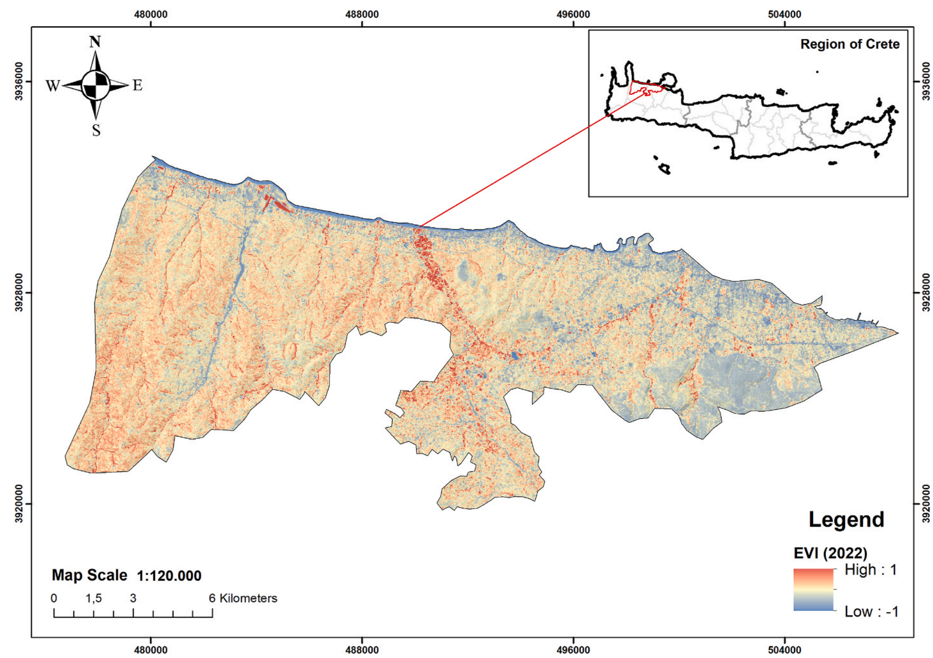

Fig. A.21. Chania Plain Enhanced Vegetation Index (EVI) map in 2022

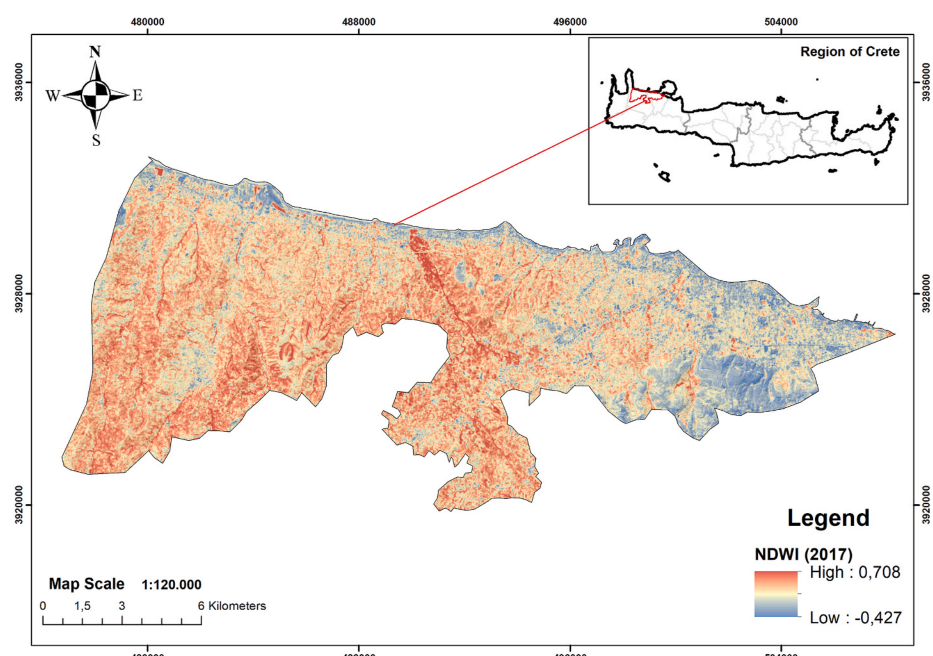

Fig. A.22. Chania Plain Normalized Difference Wetness Index (NDWI) map in 2017

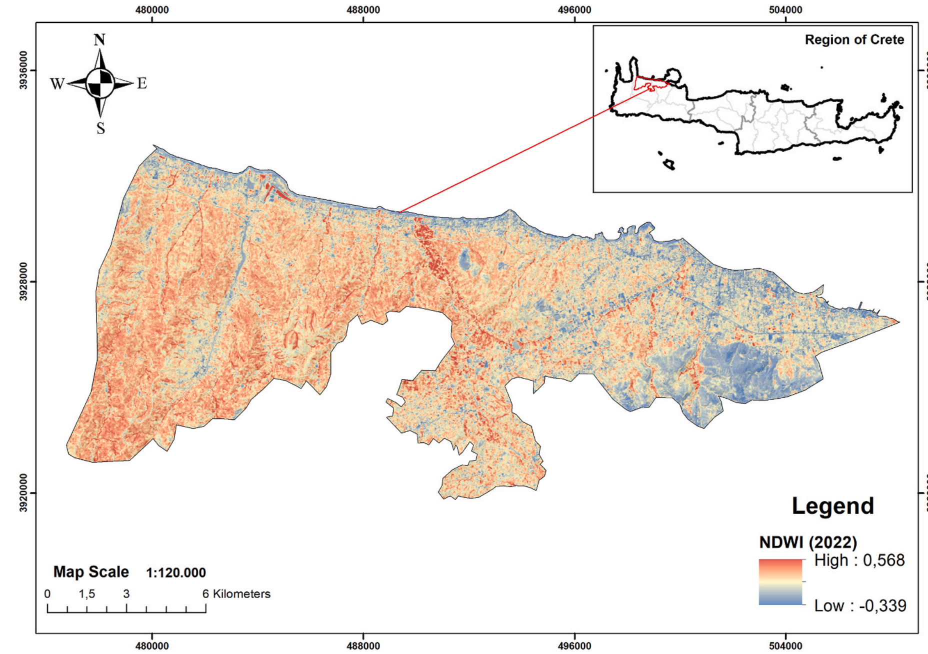

Fig. A.23. Chania Plain Normalized Difference Wetness Index (NDWI) map in 2022

Table A. 1
Criteria correlation matrix

Criteria	G	Gm	LULC	E	Sl	Ct	Prwb	Fa	Dd	Ld	TWI	TPI	TRI	R_{2017}	R_{2022}	AI_{2017}	AI_{2022}	$NDVI_{2017}$	$NDVI_{2022}$	EVI_{2017}	EVI_{2022}	$NDWI_{2017}$	$NDWI_{2022}$
G	**1.00**																						
Gm	**0.69**	**1.00**																					
LULC	-0.18	-0.23	**1.00**																				
E	-0.37	**-0.52**	0.44	**1.00**																			
Sl	-0.39	-0.44	0.35	**0.54**	**1.00**																		
Ct	0.00	-0.01	0.00	0.04	-0.01	**1.00**																	
Prwb	0.17	0.27	-0.16	-0.26	-0.15	0.01	**1.00**																
Fa	0.05	0.08	-0.01	-0.07	-0.07	-0.01	-0.04	**1.00**															
Dd	0.44	**0.52**	-0.16	-0.47	-0.34	-0.01	0.02	0.07	**1.00**														
Ld	-0.08	-0.07	0.16	0.10	0.17	0.00	0.04	-0.02	-0.08	**1.00**													
TWI	0.22	0.26	-0.13	-0.23	-0.38	0.00	0.08	0.05	0.21	-0.07	**1.00**												
TPI	0.00	-0.01	0.00	0.06	0.02	**0.57**	0.00	-0.02	-0.02	0.00	-0.01	**1.00**											
TRI	-0.41	-0.46	0.36	**0.56**	**0.98**	-0.01	-0.16	-0.07	-0.36	0.17	-0.38	0.02	**1.00**										
R_{2017}	-0.15	-0.27	-0.02	0.14	0.06	0.00	-0.20	0.00	-0.06	0.10	-0.05	0.00	0.06	**1.00**									
R_{2022}	0.06	-0.07	0.10	0.10	-0.01	0.00	-0.15	-0.02	0.02	-0.12	0.04	0.00	-0.02		**1.00**								
AI_{2017}	-0.05	-0.09	-0.02	0.11	0.02	0.00	0.01	-0.01	0.02	0.18	-0.01	0.00	0.02	**0.87**		**1.00**							
AI_{2022}	0.08	-0.04	0.11	0.10	-0.02	0.00	-0.11	-0.02	0.04	-0.11	0.05	0.00	-0.02		**0.99**		**1.00**						
$NDVI_{2017}$	-0.14	-0.22	0.15	0.11	0.06	-0.02	-0.30	0.03	0.00	-0.10	-0.02	-0.03	0.07	0.13		-0.06		**1.00**					
$NDVI_{2022}$	-0.15	-0.21	0.09	0.07	0.04	-0.02	-0.26	0.01	-0.01	-0.08	-0.02	-0.02	0.05		0.23		0.20		**1.00**				
EVI_{2017}	-0.10	-0.16	0.09	0.03	0.00	-0.02	-0.27	0.04	0.05	-0.11	0.00	-0.02	0.00	0.12		-0.06		**0.76**		**1.00**			
EVI_{2022}	-0.14	-0.18	0.04	0.05	0.02	-0.02	-0.25	0.02	-0.01	-0.08	-0.02	-0.02	0.03		0.18		0.15		**0.72**		**1.00**		
$NDWI_{2017}$	-0.18	-0.25	0.07	0.06	0.07	-0.03	-0.28	0.03	-0.05	-0.15	-0.04	-0.04	0.07	0.14		-0.09		**0.83**		**0.74**		**1.00**	
$NDWI_{2022}$	-0.21	-0.28	0.03	0.06	0.07	-0.02	-0.28	0.02	-0.08	-0.11	-0.05	-0.03	0.07		0.18		0.14		**0.77**		**0.75**		**1.00**

Table A. 2
Water table depth and pGDEz based on CRITIC weighting method for the year 2017

Monitoring station	Water table depth	pGDEz
HSGME	~34.7	High
Myloniana	~7.3	Moderate
G188	~14.7	Very high
G122	~8.1	Moderate

Data availability

Data will be made available on request.

References

Al-Abadi, A.M., Pourghasemi, H.R., Shahid, S., Ghalib, H.B., 2017. Spatial mapping of groundwater potential using entropy weighted linear aggregate novel approach and GIS. Arab. J. Sci. Eng. 42, 1185–1199. https://doi.org/10.1007/s13369-016-2374-1.

Alademomi, A.S., Okolie, C.J., Daramola, O.E., Agboola, R.O., Salami, T.J., 2020. Assessing the relationship of LST, NDVI and EVI with land cover changes in the lagos lagoon environment. Quaest. Geogr. 39 (3), 87–109. https://doi.org/10.2478/quageo-2020-0025.

Arulbalaji, P., Padmalal, D., Sreelash, K., 2019. GIS and AHP techniques based delineation of groundwater potential zones: a case study from southern Western Ghats, India. Sci. Rep. 9, 2082. https://doi.org/10.1038/s41598-019-38567-x.

Bari, E., Nipa, N.J., Roy, B., 2021. Association of vegetation indices with atmospheric & biological factors using MODIS time series products. Environ. Chall. 5, 100376. https://doi.org/10.1016/j.envc.2021.100376.

Barron, O.V., Emelyanova, I., Van Niel, T.G., Pollock, D., Hodgson, G., 2014. Mapping groundwater-dependent ecosystems using remote sensing measures of vegetation and moisture dynamics. Hydrol. Process. 28 (2), 372–385. https://doi.org/10.1002/hyp.9609.

Bhattacharya, S., Halder, S., Nag, S., Roy, P.K., Roy, M.B., 2021. Assessment of drought using multi-parameter indices. In: Roy, P.K., Roy, M.B., Pal, S. (Eds.), Advances in Water Resources Management for Sustainable Use. Lecture Notes in Civil Engineering, vol. 131. Springer, Singapore, pp. 243–255. https://doi.org/10.1007/978-981-33-6412-7_18.

Charchousi, D., Spanoudaki, K., Karali, A., Nanou-Giannarou, K., Giannakopoulos, C., Papadopoulou, M.P., 2018. An assessment approach to investigate climate change impacts in Chania groundwater system. In: XIV Internation Conference on Protection and Restoration of the Environment, 3-7 July, Thessaloniki, Greece.

Chartzoulakis, K.S., Paranychianakis, N.V., Angelakis, A.N., 2001. Water resources management in the island of Crete, Greece, with emphasis on the agricultural use. Water Policy 3, 193–205. https://doi.org/10.1016/S1366-7017(01)00012-5.

Choudhary, S., Jain, J., Pingale, S.M., Khare, D., 2023. A comprehensive review on mapping of groundwater potential zones: past, present and future recommendations. In: Balaji, E., Veeraswamy, G., Mannala, P., Madhav, S. (Eds.), Emerging Technologies for Water Supply, Conservation and Management. Springer Water. Springer, Cham, pp. 109–132. https://doi.org/10.1007/978-3-031-35279-9_6.

Diakoulaki, D., Mavrotas, G., Papayannakis, L., 1995. Determining objective weights in multiple criteria problems: the critic method. Comput. Oper. Res. 22 (7), 763–770. https://doi.org/10.1016/0305-0548(94)00059-H.

Doke, A.B., Zolekar, R.B., Patel, H., Das, S., 2021. Geospatial mapping of groundwater potential zones using multi-criteria decision-making AHP approach in a hardrock basaltic terrain in India. Ecol. Indic. 127, 107685. https://doi.org/10.1016/j.ecolind.2021.107685.

Duran-Llacer, I., Arumí, J.L., Arriagada, L., Aguayo, M., Rojas, O., González-Rodríguez, L., Rodríguez-López, L., Martínez-Retureta, R., Oyarzún, R., Singh, S.K., 2022. A new method to map groundwater-dependent ecosystem zones in semi-arid environments: a case study in Chile. Sci. Total Environ. 816, 151528. https://doi.org/10.1016/j.scitotenv.2021.151528.

Eamus, D., Froend, R., Loomes, R., Hose, G., Murray, B., 2006. A functional methodology for determining the groundwater regime needed to maintain the health of groundwater-dependent vegetation. Aust. J. Bot. 54 (2), 97–114. https://doi.org/10.1071/BT05031.

Eamus, D., Fu, B., Springer, A.E., Stevens, L.E., 2016. Groundwater dependent ecosystems: classification, identification techniques and threats. In: Jakeman, A.J., Barreteau, O., Hunt, R.J., Rinaudo, J.D., Ross, A. (Eds.), Integrated Groundwater Management. Springer, Cham, pp. 313–346. https://doi.org/10.1007/978-3-319-23576-9_13.

El-Hokayem, L., De Vita, P., Usman, M., Link, A., Conrad, C., 2023. Mapping potentially groundwater-dependent vegetation in the Mediterranean biome using global geodata targeting site conditions and vegetation characteristics. Sci. Total Environ. 898, 166397. https://doi.org/10.1016/j.scitotenv.2023.166397.

Ejaz, N., Khan, A.H., Saleem, M.W., Elfeki, A.M., Rahman, K.U., Hussain, S., Ullah, S., Shang, S., 2024. Multi-criteria decision-making techniques for groundwater potentiality mapping in arid regions: a case study of Wadi Yiba, Kingdom of Saudi Arabia. Groundw. Sustain. Dev. 26, 101223. https://doi.org/10.1016/j.gsd.2024.101223.

Evans, I.S., Cox, N.J., 1999. Relations between land surface properties: altitude, slope and curvature. In: Hergarten, S., Neugebauer, H.J. (Eds.), Process Modelling and Landform Evolution. Lecture Notes in Earth Sciences, vol. 78. Springer, Berlin, Heidelberg, pp. 13–45. https://doi.org/10.1007/BFb0009718.

Fatema, K., Joy, M.A.R., Amin, F.M.R., Sarkar, S.K., 2023. Groundwater potential mapping in Jashore, Bangladesh. Heliyon 9 (3), e13966. https://doi.org/10.1016/j.heliyon.2023.e13966.

Fildes, S.G., Doody, T.M., Bruce, D., Clark, I.F., Batelaan, O., 2023. Mapping groundwater dependent ecosystem potential in a semi-arid environment using a remote sensing-based multiple-lines-of-evidence approach. Int. J. Digit. Earth 16 (1), 375–406. https://doi.org/10.1080/17538947.2023.2176557.

Gao, B.C., 1996. Ndwi - a normalized difference water index for remote sensing of vegetation liquid water from space. Rem. Sens. Environ. 58 (3), 257–266. https://doi.org/10.1016/S0034-4257(96)00067-3.

Gao, H., Liu, F., Yan, T., Qin, L., Li, Z., 2022. Drainage density and its controlling factors on the Eastern Margin of the Qinghai–Tibet Plateau. Front. Earth Sci. 9, 755197. https://doi.org/10.3389/feart.2021.755197.

Gomes Marques, I., Nascimento, J., Cardoso, R.M., Miguéns, F., Condesso de Melo, M.T., Soares, P.M.M., Gouveia, C.M., Kurz Besson, C., 2019. Mapping the suitability of groundwater-dependent vegetation in a semi-arid Mediterranean area. Hydrol. Earth Syst. Sci. 23 (9), 3525–3552. https://doi.org/10.5194/hess-23-3525-2019.

Gou, S., Gonzales, S., Miller, G.R., 2015. Mapping potential groundwater-dependent ecosystems for sustainable management. Groundwater 53 (1), 99–110. https://doi.org/10.1111/gwat.12169.

Goumas, C., Dokou, Z., Morianou, G.G., Kourgialas, N.N., Karatzas, G.P., 2017. Using Groundwater Flow Simulation of the Chania Plain Area to Propose a Proper Irrigation Plan, vol. 57. European Water, pp. 467–473.

Guhananth, K., Gomes, P.I.A., Abeysiriwardana, H.D., 2023. GIS-based landslide susceptibility mapping: a case study from Kegalle District, Sri Lanka. In: Das, J., Bhattacharya, S.K. (Eds.), Monitoring and Managing Multi-Hazards. GIScience and Geo-Environmental Modelling. Springer, Cham, pp. 197–210. https://doi.org/10.1007/978-3-031-15377-8_13.

Habib, M., 2021. Quantifying topographic ruggedness using principal component analysis. Adv. Civ. Eng. 2021 (1), 3311912. https://doi.org/10.1155/2021/3311912.

Hairchi, K.E., Limame, A., Benbrahim, Y., Saadi, O., Ouiaboub, L., Nouayti, A., Nouayti, N., 2024. Groundwater potential zones mapping using GIS, RS, and AHP method in the Guigou basin, Middle Atlas, Morocco. Euro-Mediterr. J. Environ. Integr. https://doi.org/10.1007/s41207-024-00607-y.

Howard, J., Merrifield, M., 2010. Mapping groundwater dependent ecosystems in California. PLoS One 5 (6), e11249. https://doi.org/10.1371/journal.pone.0011249.

Howard, J.K., Dooley, K., Brauman, K.A., Klausmeyer, K.R., Rohde, M.M., 2023. Ecosystem services produced by groundwater dependent ecosystems: a framework and case study in California. Front. Water. 5, 1115416. https://doi.org/10.3389/frwa.2023.1115416.

Huang, S., Tang, L., Hupy, J.P., Wang, Y., Shao, G., 2021. A commentary review on the use of normalized difference vegetation index (NDVI) in the era of popular remote sensing. J. For. Res. 32, 1–6. https://doi.org/10.1007/s11676-020-01155-1.

Hulluka, T.A., Ebrahim, G.Y., Haile, A.T., Haileslassie, A., 2024. Shallow groundwater potential mapping and evaluation for climate resilient small holder irrigation in the Zeway-Shalla sub-Basin, Ethiopia. Groundw. Sustain. Dev. 23, 101367. https://doi.org/10.1016/j.gsd.2024.101367.

Jahan, A., Mustapha, F., Sapuan, S.M., Ismail, M.Y., Bahraminasab, M., 2012. A framework for weighting of criteria in ranking stage of material selection process. Int. J. Adv. Manuf. Technol. 58, 411–420. https://doi.org/10.1007/s00170-011-3366-7.

Jhariya, D.C., Khan, R., Mondal, K.C., Kumar, T., Indhulekha, K., Singh, V.K., 2021. Assessment of groundwater potential zone using GIS-based multi-influencing factor (MIF), multi-criteria decision analysis (MCDA) and electrical resistivity survey techniques in Raipur city, Chhattisgarh, India. Aqua Water Infrastruct. Ecosyst. Soc. 70 (3), 375–400. https://doi.org/10.2166/aqua.2021.129.

Kabeto, J., Adeba, D., Regasa, M.S., Leta, M.K., 2022. Groundwater potential assessment using GIS and remote sensing techniques: case study of west Arsi zone, Ethiopia. Water 14 (12), 1838. https://doi.org/10.3390/w14121838.

Kolitsi, G., Charchousi, D., Mellios, N.K., Papadopoulou, M.P., 2024. Mapping groundwater dependent ecosystems for sustainable management of aquifers. In: Eleventh International Conference on Environmental Management, Engineering, Planning & Economics, 16-20 June, Lefkada Island, Greece.

Krishnan, A.R., Kasim, M.M., Hamid, R., Ghazali, M.F., 2021. A modified CRITIC method to estimate the objective weights of decision criteria. Symmetry 13 (6), 973. https://doi.org/10.3390/sym13060973.

Kourgialas, N.N., Koubouris, G.C., Dokou, Z., 2019. Optimal irrigation planning for addressing current or future water scarcity in Mediterranean tree crops. Sci. Total Environ. 654, 616–632. https://doi.org/10.1016/j.scitotenv.2018.11.118.

Kritikakis, G., Kokinou, E., Economou, N., Andronikidis, N., Brintakis, J., Daliakopoulos, I.N., Kourgialas, N., Pavlaki, A., Fasarakis, G., Markakis, N., Soupios, P., Manios, T., Vafidis, T., 2022. Estimating soil clay content using an agrogeophysical and agrogeological approach: a case study in Chania Plain, Greece. Water 14 (17), 2625. https://doi.org/10.3390/w14172625.

Li, S., Abdelkareem, M., Al-Arifi, N., 2023. Mapping groundwater prospective areas using remote sensing and GIS-based data driven frequency ratio techniques and detecting land cover changes in the yellow river basin, China. Land 12 (4), 771. https://doi.org/10.3390/land12040771.

Liu, C., Liu, H., Yu, Y., Zhao, W., Zhang, Z., Guo, L., Yetemen, O., 2021. Mapping groundwater-dependent ecosystems in arid Central Asia: implications for controlling regional land degradation. Sci. Total Environ. 797, 149027. https://doi.org/10.1016/j.scitotenv.2021.149027.

Luijendijk, E., 2022. Transmissivity and groundwater flow exert a strong influence on drainage density. Earth Surf. Dynam. 10 (1), 1–22. https://doi.org/10.5194/esurf-10-1-2022.

Lykhovyd, P., Averchev, O., Fedorchuk, M., Fedorchuk, V., 2023. The relationship between spatial vegetation indices: a case study for the south of Ukraine. Environ. Ecol. Res. 11 (5), 740–746. https://doi.org/10.13189/eer.2023.110504.

Martínez-Santos, P., Díaz-Alcaide, S., De la Hera-Portillo, A., Gómez-Escalonilla, V., 2021. Mapping groundwater-dependent ecosystems by means of multi-layer supervised classification. J. Hydrol. 603, 126873. https://doi.org/10.1016/j.jhydrol.2021.126873.

Mattivi, P., Franci, F., Lambertini, A., Bitelli, G., 2019. TWI computation: a comparison of different open source GISs. Open geospatial data, softw. stand. 4, 6. https://doi.org/10.1186/s40965-019-0066-y.

Meng, F., Liang, X., Xiao, C., Wang, G., 2021. Integration of GIS, improved entropy and improved catastrophe methods for evaluating suitable locations for well drilling in arid and semi-arid plains. Ecol. Indic. 131, 108124. https://doi.org/10.1016/j.ecolind.2021.108124.

Mhlanga, S.T., Lall, M., 2022. Influence of normalization techniques on multi-criteria decision-making methods. J. Phys: Conf. Ser. 2224, 012076. https://doi.org/10.1088/1742-6596/2224/1/012076.

Middleton, N., Thomas, D. (Eds.), 1992. World Atlas of Desertification. Edward Arnold, London.

Minár, J., Evans, I.S., Jenčo, M., 2020. A comprehensive system of definitions of land surface (topographic) curvatures, with implications for their application in geoscience modelling and prediction. Earth Sci. Rev. 211, 103414. https://doi.org/10.1016/j.earscirev.2020.103414.

Morianou, G., 2014. Identification of Accumulation Areas of Surface Runoff in the River Basin Tavronitis (Chania Prefecture) Using the Model MIKE SHE. Technical University of Crete, Dissertation (in Greek).

Mukhametzyanov, I., 2021. Specific character of objective methods for determining weights of criteria in MCDM problems: entropy, CRITIC and SD. Decis. Mak. Appl. Manag. Eng. 4 (2), 76–105. https://doi.org/10.31181/dmame210402076i.

Münch, Z., Conrad, J., 2007. Remote sensing and GIS based determination of groundwater dependent ecosystems in the Western Cape, South Africa. Hydrogeol. J. 15, 19–28. https://doi.org/10.1007/s10040-006-0125-1.

Nerantzaki, S.D., Nikolaidis, N.P., 2020. The response of three Mediterranean karst springs to drought and the impact of climate change. J. Hydrol. 591, 125296. https://doi.org/10.1016/j.jhydrol.2020.125296.

Odu, G.O., 2019. Weighting methods for multi-criteria decision making technique. J. Appl. Sci. Environ. Manag. 23 (8), 1449–1457. https://doi.org/10.4314/jasem.v23i8.7.

Pandey, H.K., Singh, V.K., Singh, S.K., Sharma, S.K., 2023. Mapping and validation of groundwater dependent ecosystems (GDEs) in a drought-affected part of Bundelkhand region, India. Groundw. Sustain. Dev. 23, 100979. https://doi.org/10.1016/j.gsd.2023.100979.

Prountzos, S., 2013. Characterization of Lakes and Surface Water Bodies in Western Crete Based on the Framework Directive 2000/60/EC. National Technical University of Athens, Dissertation (in Greek).

Qu, W., Li, J., Song, W., Li, X., Zhao, Y., Dong, H., Wang, Y., Zhao, Q., Qi, Y., 2022. Entropy-weight-method-based integrated models for short-term intersection traffic flow prediction. Entropy 24 (7), 849. https://doi.org/10.3390/e24070849.

Rai, P.K., Mohan, K., Mishra, S., Ahmad, A., Mishra, V.N., 2017. A GIS-based approach in drainage morphometric analysis of Kanhar River Basin, India. Appl. Water Sci. 7, 217–232. https://doi.org/10.1007/s13201-014-0238-y.

Rampheri, M.B., Dube, T., Dondofema, F., Dalu, T., 2023. Identification and delineation of groundwater-dependent ecosystems (GDEs) in the Khakea–Bray transboundary aquifer region using geospatial techniques. Geocarto Int. 38 (1), 2172217. https://doi.org/10.1080/10106049.2023.2172217.

Riley, S.J., DeGloria, S.D., Elliot, R., 1999. A terrain ruggedness index that quantifies topographic heterogeneity. Intermountain J. Sci. 5 (1–4), 23–27.

Rohde, M.M., Albano, C.M., Huggins, X., Klausmeyer, K.R., Morton, C., Sharman, A., Zaveri, E., Saito, L., Freed, Z., Howard, J.K., Job, N., Richter, H., Toderich, K., Rodella, A.S., Gleeson, T., Huntington, J., Chandanpurkar, H.A., Purdy, A.J., Famiglietti, J.S., Singer, M.B., Roberts, D.A., Caylor, K., Stella, J.C., 2024. Groundwater-dependent ecosystem map exposes global dryland protection needs. Nature 632, 101–107. https://doi.org/10.1038/s41586-024-07702-8.

Şahin, M.A., 2021. Comprehensive analysis of weighting and multicriteria methods in the context of sustainable energy. Int. J. Environ. Sci. Technol. 18, 1591–1616. https://doi.org/10.1007/s13762-020-02922-7.

Shannon, C.E., 1948. A mathematical theory of communication. Bell System. Tech. J. 27 (3), 379–423. https://doi.org/10.1002/j.1538-7305.1948.tb01338.x.

Soupios, P.M., Kouli, M., Vallianatos, F., Vafidis, A., Stavroulakis, G., 2007. Estimation of aquifer hydraulic parameters from surficial geophysical methods: a case study of Keritis Basin in Chania (Crete– Greece). J. Hydrol. 338, 122–131. https://doi.org/10.1016/j.jhydrol.2007.02.028.

Steiakakis, E., Vavadakis, D., Mourkakou, O., 2023. Groundwater vulnerability and delineation of protection zones in the discharge area of a karstic aquifer—application in agyia's karst system (Crete, Greece). Water 15 (2), 231. https://doi.org/10.3390/w15020231.

Strashok, O., Ziemiańska, M., Strashok, V., 2022. Evaluation and correlation of normalized vegetation index and moisture index in kyiv (2017–2021). J. Ecol. Eng. 23 (9), 212–218. https://doi.org/10.12911/22998993/151884.

Thornthwaite, C.W., 1948. An approach toward a rational classification of climate. Geogr. Rev. 38 (1), 55–94. https://doi.org/10.2307/210739.

Trevisani, S., Teza, G., Guth, P.L., 2023. Hacking the topographic ruggedness index. Geomorphology 439, 108838. https://doi.org/10.1016/j.geomorph.2023.108838.

Xu, W., Kong, F., Mao, R., Song, J., Sun, H., Wu, Q., Liang, D., Bai, H., 2022. Identifying and mapping potential groundwater-dependent ecosystems for a semi-arid and semi-humid area in the Weihe River, China. J. Hydrol. 609, 127789. https://doi.org/10.1016/j.jhydrol.2022.127789.

Zewdie, M.M., Kasie, L.A., Bogale, S., 2024. Groundwater potential zones delineation using GIS and AHP techniques in upper parts of Chemoga watershed, Ethiopia. Appl. Water Sci. 14, 85. https://doi.org/10.1007/s13201-024-02119-0.

Web references

Copernicus Data Space Ecosystem, 2024. https://dataspace.copernicus.eu (Accessed 20 September 2024).

ESRI, 2024. ArcGIS Desktop. https://www.esri.com/en-us/arcgis/products/arcgis-desktop/overview. (Accessed 20 September 2024).

FILOTIS, 2024. Database for the natural environment of Greece. https://filotis.itia.ntua.gr/biotopes/c/GR4340006/. (Accessed 20 September 2024).

Geoportal of Greek Ministry of environment and energy. https://mapsportal.ypen.gr, 2024–. (Accessed 20 September 2024) (in Greek).

Greek Ministry of Environment and Energy, 2024. Hydrogeological map of Greece. https://ypen.gov.gr/wp-content/uploads/2023/10/υδρολιθολογικός-Ελλάδας.pdf. (Accessed 20 September 2024) (in Greek).

Hellenic Republic, Ministry of Environment & Energy, Special Secretariat for water, 2024. 1st revision of river basin management plan for the Crete river basin district (EL13) summary. https://wfdver.ypeka.gr/wp-content/uploads/2021/02/EL13_1REV_P22b_Perilipsi_EN.pdf. (Accessed 20 September 2024).

U.S. Geological Survey, 2024. Landsat missions. Landsat enhanced vegetation index. https://www.usgs.gov/landsat-missions/landsat-enhanced-vegetation-index. (Accessed 20 September 2024).

Sharma, A., Patel, P.L., 2024. Exploring the dependency between climatic variables and aridity index in a semi-arid Basin in India. National Water Development Agency. https://www.nwda.gov.in/upload/uploadfiles/e-book/S-3/Exploring-the-dependency-between-climatic.pdf. (Accessed 20 September 2024).

Geoportal of Decentralized Administration of Crete,, 2024. (in Greek). https://geoportal.apdkritis.gov.gr (Accessed 20 September 2024).